Environmental Science Advances

TUTORIAL REVIEW

View Article Online
View Journal

Cite this: DOI: 10.1039/d6va00059b

Towards sustainable photocatalytic degradation of organic pollutants through rational design of engineered magnetically retrievable metal oxide@graphene oxide nanocomposites

Kirti,[a] Anju Srivastava, *[a] Sriparna Dutta,*[a] R. K. Sharma, [b] Reena Jain,[a] Prashant Kumar, [c] Ruchi Singh,[a] Priyanka,[a] Vipin Kumar Upadhyay,[d] Geetanshu[a] and Siddharth N. Kurur[e]

Toxic pollutants in aqueous media cause great harm to both the environment and living beings; thus, the remediation of such pollutants through the design and development of highly efficient and recyclable nanomaterials is pivotal. These nanoscale platforms enable superior adsorption and catalytic performance while minimizing energy input and secondary waste compared to conventional treatment technologies. Among the various nanomaterials investigated, magnetically retrievable graphene oxide nanocomposites have emerged as highly promising candidates for the remediation of a large array of pollutants, including heavy metals and organic contaminants such as dyes, pesticides, herbicides, and pharmaceuticals. The outstanding performance of such nanocomposites is attributed to their high specific surface area, which enables increased adsorption capacity, superior degradation efficiency, excellent stability, ease of magnetic separation, facile modification and functionalization. Furthermore, recent studies have demonstrated that coupling semiconducting metal oxides with graphene oxide-based nanocomposites yields photoactive materials with tailored band gaps, capable of harnessing solar or visible light for photocatalytic degradation, thereby providing an affordable, efficient, and sustainable strategy for treating air and water contamination. This review examines the synthesis and functionalization of such nanomaterials, with particular emphasis on their photocatalytic pollutant removal mechanisms. By integrating mechanistic insights with application-oriented considerations, this work offers a cohesive framework for the rational design of sustainable, reusable, and efficient nanomaterials for environmental remediation and water purification. In doing so, it bridges fragmented research efforts, highlights future research directions, and provides actionable insights for translating laboratory innovations into real-world environmental remediation solutions.

Received 4th February 2026
Accepted 6th April 2026

DOI: 10.1039/d6va00059b

rsc.li/esadvances

Environmental significance

The review focuses on the rational design of magnetic metal oxide@graphene oxide (MMO@GO) based nanocomposites, especially with regard to their role in the sustainable photocatalytic degradation of a plethora of organic pollutants-including pharmaceuticals, such as antimicrobials, antipyretics, antidiabetics, *etc.*, microplastics, dyes and pesticides. This work significantly aligns with various UN Sustainable Development Goals by promoting visible light driven photocatalysis, high reusability and minimum secondary waste generation.

1. Introduction

Industrialization has played a pivotal role in the development of modern society by revolutionizing every aspect of human life. With the huge benefits and comforts industrialization has brought to our civilization, it is also the reason for the large-scale destruction of the earth's natural environment.[1] Pollutants such as heavy metals, organic pollutants, emerging micro-contaminants, *etc.* and products released from industrial processes lead to the contamination of our natural resources, including air, water, and soil. This has made air unbreathable, water undrinkable, and soil unfit for cultivation, leading to various diseases and environmental concerns such as cancer, asthma, heart and brain diseases, and global warming.[2,3] Organic pollutants in particular are one of the major causes of water and air pollution.[4,5]

[a]*Department of Chemistry, Hindu College, University of Delhi, Delhi 110007, India. E-mail: dr.anjusrivastava@gmail.com*
[b]*Green Chemistry Network Centre, Hindu College, University of Delhi, Delhi 110007, India*
[c]*Department of Chemistry, SRM University Delhi-NCR, Sonepat, Haryana 131029, India*
[d]*Department of Chemistry, IIT Kanpur, Kanpur 208016, India*
[e]*Department of Chemistry, University of Delhi, Delhi 110007, India*

The World Health Organization (WHO) claims that even low concentrations of these persistent organic pollutants (POPs) can cause harmful health effects, such as a higher risk of cancer, compromised immune response, neurological effects, endocrine disruption, genotoxicity, and congenital disorders. Therefore, targeting these POPs becomes an essential part of combating environmental pollution. With the current demand to combat these critical issues, numerous efforts have been made by researchers to capture and eliminate these pollutants from the environment using many techniques ranging from the simplest filtration-based methods to the most sophisticated methods involving artificial intelligence (AI).[6–9] The current techniques are either not efficient enough or unaffordable or are not eco-friendly, making them unsuitable for large-scale application.[9]

Photocatalysts have the ability to absorb light and produce reactive oxygen species (ROS) (Fig. 1). ROS, including $^{\bullet}OH$ and $O_2^{\bullet-}$, cause deterioration of pollutants through a redox mechanism. The process employs light activated semi-conductor catalysts to generate reactive oxygen species (ROS) that oxidize contaminants.[10] When the catalyst's surface is exposed to light with an energy equivalent to or greater than its band gap, excitation of electrons occurs from the valence band to the conduction band generating holes in the valence band, resulting in the formation of electron hole (e^-/h^+) pairs. ROS are produced when the electron–hole pairs interact with oxygenated species on the catalyst's surface, such as water and air. $O_2^{\bullet-}$ is created by the electron through dissolved oxygen reduction, whereas $^{\bullet}OH$ is produced when water is oxidized by a hole. When $O_2^{\bullet-}$ reacts with H_2O, it produces H_2O_2 and increases the synthesis of $^{\bullet}OH$. Although the degradation process achieves high efficiency in general, the efficiency of a specific nanocomposite is determined by several factors that can influence the formation of reactive radicals such as catalyst concentration, pharmaceutical concentration, dissolved oxygen levels, pH, water matrix, oxidant concentration, light source, and intensity.[11–16]

Metal oxides are considered promising candidates as photocatalysts owing to their low cost, high efficiency, simple synthesis routes, and sufficient availability (Fig. 2).[17,18] However due to their wide band gap they require UV light to serve as a photocatalyst that limits their usage.[19] When graphene oxide is coupled with metal oxides, it inhibits the recombination of photogenerated (e^-/h^+) pairs enhancing the overall catalytic activity.[20] It also reduces the band gap of these metal oxides

Kirti

Kirti is a research scholar currently working under the supervision of Prof. Anju Srivastava at the Department of Chemistry, Hindu College, University of Delhi. She completed her post-graduation at SRM University in 2019 and her graduation at Maharshi Dayanand University in 2017. She qualified for the prestigious Junior Research Fellowship awarded by the Council of Scientific and Industrial Research (CSIR), New Delhi, India. She has published several research articles in reputed journals of the Royal Society of Chemistry (RSC) and the American Chemical Society (ACS). In recognition of the quality of her research and presentation skills, she has also received the Best Presentation Award at an international conference. Her research interests focus on the design and development of engineered photocatalysts for wastewater remediation and environmental sustainability.

Anju Srivastava

Prof. Anju Srivastava is a Professor of Chemistry and Principal of a premier institution ranked amongst the top three in the country, Hindu College, University of Delhi. She received her MSc and PhD in Synthetic Polymer Chemistry from IIT Delhi and has a teaching experience of 30 years in the subject areas of organic chemistry, biochemistry, environmental chemistry and analytical chemistry. Furthermore, she is co-editor of several books and has been nominated as a Fellow at ILLL (Institute of Lifelong Learning) University of Delhi and conferred with the 'Distinguished Teacher' Award by the former President of India, Dr A. P. J. Abdul Kalam. She has several publications in reputed international journals to her credit including Materials Horizons, Materials Advances, Dalton Transactions and many more.

Sriparna Dutta

Dr. Sriparna Dutta is an Assistant Professor at Hindu College, Department of Chemistry, University of Delhi. In the past, she has served the role of secretary of the ACS Student Chapter, D.U., and has been instrumental in organizing diverse activities as an active member of the Green Chemistry Network Centre, D.U. Her research domain centers broadly around the fabrication of core–shell nanomaterials for diverse catalytic applications that have credited her with important publications in reputed international journals including Chemical Society Reviews, Green Chemistry, ACS Omega, Dalton Transactions, Materials Chemistry Frontiers, etc. *She has also authored several book chapters in Elsevier, the RSC Green Chemistry Series, World Scientific Publications,* etc.

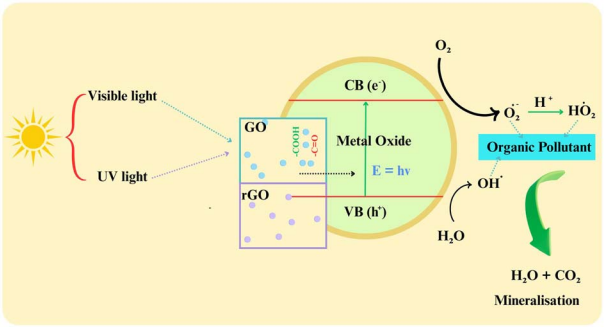

Fig. 1 Schematic representation of formation of ROS under UV and visible light irradiation on a photocatalyst.

further enhancing their catalytic activity.[21,22] GO nanocomposites possess the appropriate band gap required to harness solar energy or light for their photocatalytic activity, thereby making them an affordable, effective, and sustainable solution to treat air and water contamination.[23,24]

Graphene and graphene oxide (GO) based materials have been employed in diverse domains such as hydrogen storage, harmful gas removal, biomedical applications, *etc.* because of their unique physicochemical characteristics, including extensive active surface area and high operational efficiency.[25,26] Researchers have reported that graphene oxide exhibits superior oxidizing properties compared to graphene because it carries oxygen rich functional groups such as hydroxyl (–OH), carboxyl (–COOH), and epoxy (–COC) groups. Thus, its processing and synthesis become easier, making it more suitable for application. GO has been found to be a good candidate for the treatment of water; however its high dispersibility prevents easy separation from water after the adsorption of pollutants.[27–29] To overcome this challenge, researchers have developed methods to magnetize GO by attaching magnetic moieties on its surface, enabling its easy separation from water using an external magnetic field and allowing for reuse. Thus, magnetic graphene oxide-based nanocomposites are gaining popularity now a days in eliminating toxic pollutants like heavy metals and organic pollutants, including dyes, pesticides, herbicides, and pharmaceuticals owing to their unique physicochemical properties, such as strong magnetic and photocatalytic performances, large surface-active sites and surface area, high chemical stability, remarkable efficiency, good control of their morphological characteristics, and the ease with which they can be functionalized.[30–33]

2. Scope of the review

The review compiles recent advances in sustainable, magnetically retrievable photocatalytic nanocomposites for the efficient degradation of hazardous organic pollutants in water, aligning with the United Nations Sustainable Development Goal 6 (Clean Water and Sanitation), which aims to ensure safe and clean water for all. The rational design of reusable metal oxide@graphene oxide photocatalysts promotes environmentally friendly and energy-efficient wastewater treatment technologies that support global water quality improvement objectives.[34,35] It seeks to present an extensive overview of magnetic metal oxide@graphene oxide (MMO@GO) based nanocomposites, emphasizing their synthesis, physicochemical properties, and role in photocatalytic degradation of organic pollutants. A

R. K. Sharma

Prof. R. K. Sharma is the Director of the Green Chemistry Network Centre, Hindu College, University of Delhi, India, a fellow of the Royal Society of Chemistry (RSC) and the Honorary Secretary of RSC London (North India Section). He is also Honorary Professor at Deakin University, Australia. Prof. Sharma worked on a JSPS PDF at the University of Tokyo and Kumamoto University. He has published more than 250 research and review articles in renowned international journals which include the top cited articles of Chemical Society Reviews, Green Chemistry, Materials Horizons and Nature Scientific Reports. Currently he is the series advisor of the RSC Green Chemistry Book Series and a member of the editorial board of Current Research in Green and Sustainable Chemistry. He has edited and authored several books on Green Chemistry published by the RSC green chemistry series, Stanford, Wiley and World Scientific Publications. Recently, he has been conferred the Most Cited Researcher by the Royal Society of Chemistry.

Reena Jain

Prof. Reena Jain is the Vice-Principal of Hindu College and a Professor in the Department of Chemistry, Hindu College University of Delhi. She has an extensive teaching experience of more than 25 years. Besides teaching, Prof. Reena Jain has been actively involved in various research assignments and projects as the co-supervisor and co-principal investigator, providing necessary guidance and support to the students working on MSc dissertation/innovation projects under her supervision. Her areas of research interest include Inorganic Chemistry, Organometallic Chemistry, Green Chemistry, Analytical Chemistry and Environmental Chemistry. Prof. Jain has also authored/co-authored a number of research publications in peer-reviewed journals and books for school and college students besides being involved in the development of e-content, video lectures, etc.

Fig. 2 Different metal oxides which are popularly being used for making nanocomposites.

detailed overview of the fabrication methodologies implemented for producing MMO@GO hybrid nanomaterials, including co-precipitation, hydrothermal, and green synthesis techniques has been discussed. Insights into the utilization of MMO@GO and MMO@rGO (magnetic metal oxide@graphene oxide and magnetic metal oxide@reduced graphene oxide) nanocomposites in environmental remediation, particularly for the removal of organic pollutants including dyes, pesticides, pharmaceuticals and microplastics from aqueous solutions, have been elaborated. A critical comparison of the magnetic metal oxide anchored graphene oxide nanocomposites has been made with the other reported photocatalysts taking into account all important parameters involved in assessing the quality of a catalyst. Lastly, current limitations and challenges in the field, along with proposed solutions and future research directions aimed at advancing the practical applications of MMO@GO based nanocomposites, are addressed.

Although, until now, a number of review articles have been penned focusing on photocatalytic materials for the remediation of wastewater contaminated with organic pollutants, limited attention has been paid to the rational design, functionality, and potential of metal oxide-anchored magnetically retrievable graphene oxide nanocomposites. It is expected that the rational design of such nanocomposites will provide a potential photocatalytic material for the efficient degradation of organic pollutants. With this background, this review article provides a comprehensive overview of the design strategies, mechanistic understanding, and recent developments in the design of MMO@GO nanocomposites for the efficient degradation of organic pollutants. It is expected that this compilation will help the scientific community in harnessing the potential of such nanocomposites in the future.

Lastly, current limitations and challenges in the field, along with proposed solutions and future research directions aimed at advancing the practical applications of MMO@GO based nanocomposites are addressed. Through this review we aim to provide support to researchers and practitioners to explore and utilize the potential of MMO@GO based nanocomposites across scientific and industrial sectors.

3. Synthesis of magnetic metal oxide@graphene oxide based nanocomposites

3.1 Synthesis of GO@ZnO@Fe_3O_4 and related nanocomposites

Metal oxides are utilized as components of photocatalytic systems due to their wide band-gaps and resistance to photocorrosion. Zinc oxide (ZnO) is a popular choice due to its very wide band-gap, low cost, high photocatalytic activity, and high chemical stability.[36] A key component among many of these hybrid systems is graphene oxide, generally synthesized through Hummers' method or its modified approaches. The classical Hummers' method was introduced in 1957 by William S Hummers, Jr. which offers a safer, faster alternative to the Staudenmaier Hofmann-Hamdi's method involving a laborious and dangerous synthetic pathway due to the use of potassium chlorate in the presence of concentrated H_2SO_4 and HNO_3. Hummers' method[37] replaces these reagents with a water free mixture of concentrated H_2SO_4, sodium nitrate and potassium permanganate to oxidize graphite. In contrast the modified Hummers' method described by Marcano *et al.*[38] eliminates the use of $NaNO_3$ and employs a 9 : 1 mixture of H_2SO_4 and H_3PO_4.

In 2020, Abbasi and co-workers[39] prepared Fe_3O_4@ZnO@GO nanocomposites and evaluated their photocatalytic performances towards the degradation of organic dye pollutants. A hydrothermal procedure was used to synthesise Fe_3O_4 nanoparticles. $Fe(acac)_3$ was dispersed into ethylene glycol, followed by addition and mixing of NH_4Ac. The reaction mixture was heated at 200 °C for 24 h before being cooled to room temperature. The synthesized compound was filtered, washed and dried at 60 °C for 12 h. For the synthesis of GO@Fe_3O_4, a similar process was followed with the incorporation of GO followed by agitation using an ultrasound bath. The synthesized product was separated from the suspension using an external magnetic field. For synthesizing GO@Fe_3O_4@ZnO nanocomposites, GO@Fe_3O_4 particles were dispersed in distilled water and agitated using an ultrasound bath, following which $ZnCl_2$ was dissolved in the solution. The solution was heated to 90 °C and NaOH solution was added dropwise under vigorous agitation. The powder obtained was separated, washed and dried at 80 °C for 12 h and calcined at 300 °C.

In parallel but with different intent, Eivazzadeh-Keihan *et al.* synthesized melamine functionalized Fe_3O_4@ZnO@GO nanocomposites and studied their use in organic catalysis and electrical capacitance. Graphene oxide nanosheets (GONSs) were first activated with DCC and subsequently functionalized with melamine under ultrasonication (Fig. 3). The resulting mixture was stirred at room temperature, centrifuged, and washed with ethanol. Next, a solution of iron chloride salts in deionized water was combined with the melamine-functionalized GONSs. After that, Fe_3O_4 nanoparticles were synthesized and intercalated through an *in situ* codeposition process carried out at a pH of 12 under neutral atmospheric conditions. The obtained Fe_3O_4@GO@melamine nanoparticles were dispersed in deionized water, followed by the addition of

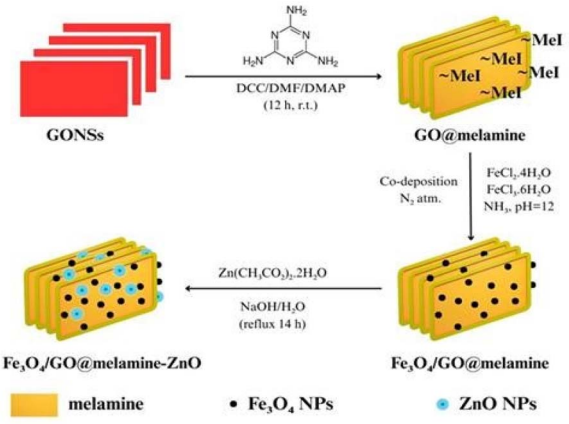

Fig. 3 Schematic representation of an Fe_3O_4@GO@melamine-ZnO nanocomposite.

zinc acetate and sodium hydroxide, and the mixture was stirred for 1 h. The mixture was then subjected to vigorous stirring under reflux for 14 h. Finally, the synthesized nanocomposites were isolated using an external magnet, thoroughly washed, and dried at 60 °C.[40]

Using magnesium ferrite as a magnetic material, Bateni and coworkers[41] synthesized pectin/GO@$MgFe_2O_4$@ZnO nanocomposites to study the photocatalytic degradation of aqueous solution of diclofenac. GO nanosheets were prepared using modified Hummers' method, while ZnO nanoparticles were synthesized by mixing aqueous solutions of NaOH and zinc nitrate and refluxing at 90 °C. Aqueous solutions of iron nitrate and magnesium nitrate were mixed and the synthesized ZnO nanoparticles were immersed with constant stirring. The resulting mixture was added slowly to NaOH solution, following which it was sealed at 90 °C. Once cooled, the product was washed, centrifuged and dried at 80 °C and then calcined at 500 °C. A pectin@GO nanocomposite was synthesized with the help of DMAP and DCC as catalysts followed by addition of ZnO@$MgFe_2O_4$ nanoparticles and stirring for 48 h under ultrasonication. Centrifugation of the suspension and subsequent washing and drying yielded the required photocatalyst. Extending the applicability towards biomedical technology, Salimi *et al.* synthesized Fe_3O_4@ZnO@GO nanocomposites for drug delivery applications. Hummers' method was used to synthesize graphene oxide. Magnetic (Fe_3O_4) nanoparticles were synthesized *via* thermal treatment by mixing iron(II) nitrate and iron(III) nitrate in a solution with polyvinylpyrrolidone (PVP). To synthesize Fe_3O_4@ZnO nanocrystals, iron oxide nanoparticles and zinc nitrate were mixed in an aquatic environment before synthesizing Fe_3O_4@ZnO@GO nanocomposites.[42]

3.2 Synthesis of GO@TiO_2@Fe_3O_4 and related nanocomposites

TiO_2 is abundant, non-toxic, and environmentally benign, which has made it a widely studied material for environmental applications.[43,44] Over the past decade numerous TiO_2@-GO@magnetic hybrid nanocomposites have been engineered to improve its catalytic properties. Cao *et al.* reported one of the earlier advancements in the field with the development of a magnetically separable graphene-TiO_2 ($MGTiO_2$) hybrid photocatalyst *via* a one-step method.[45] Modified Hummers' method was used to synthesized graphene oxide (GO) while a co-precipitation method was used to synthesize Fe_3O_4 nanoparticles. The two solutions were mixed in a 1 : 1 weight ratio under continuous stirring for 1 h which resulted in the formation of MGO composites. Subsequently titania coated MGO composites were synthesized through a solvothermal approach using tetrabutyl titanate. The crystalline structure of the obtained samples was characterized by XRD while the band gaps of MGO-TiO_2 with TiO_2 loadings of 0.5%, 1%, 3%, and 5% were reported to be 3.15, 3.14, 3.11 and 3.06 eV, respectively.

Building on this concept, Li *et al.* synthesized TiO_2@-graphene@Fe_3O_4 nanocomposites.[46] GO was synthesized *via* Hummers' method while anatase TiO_2 was prepared using hydrolysis and hydrothermal treatment of $Ti(BuO)_4$, and both were incorporated to form TiO_2@GO. To it, acid-resistant Fe_3O_4 nanoparticles were introduced to mitigate Fe(II) leaching. TiO_2 is mixed with potassium hydroxide (KOH) and potassium nitrate (KNO_3), followed by $FeSO_4$ under nitrogen purging. The mixture underwent hydrothermal treatment at 90 °C, resulting in the formation of TiO_2@graphene@Fe_3O_4.

In the same year, Ghosh *et al.* engineered TiO_2@$CoFe_2$-O_4@rGO nanocomposites[47] *via* a non-hydrothermal, water-based route. The method avoids the use of high-pressure autoclaves and organic solvents. $CoFe_2O_4$ nanoparticles were prepared using an EFT assisted method, while incorporation of TiO_2 occurred *via* a surfactant-assisted sol–gel process. GO was synthesized by employing Hummers' method and was reduced to RGO using hydrazine. TiO_2@$CoFe_2O_4$ with dispersed GO was refluxed followed by chemical reduction and drying, yielded the final nanocomposites with a band gap of 2.22 eV and strong magnetic properties (M_s: 14.5 emu per g).

Continuing advancement in multifunctional photocatalytic systems, Qilong Li and co-workers synthesized TiO_2-GO-Fe_3O_4 nanocomposites[48] through a multi-step fabrication approach with enhanced photo-Fenton catalysis and magnetic recovery. GO was prepared *via* Hummers' method and TiO_2 was incorporated through hydrothermal treatment at 120 °C while the incorporation of Fe_3O_4 was achieved by mixing $Fe(NO_3)_3 \cdot 9H_2O$ in the former Go-TiO_2 solution followed by ultrasonic treatment, drying, and alkaline treatment at 180 °C. Reduction with ethylene glycol converted $Fe(OH)_3$ formed due to alkaline treatment to Fe_3O_4; subsequently the composite was vacuum dried. The design improves charge separation, photocatalytic efficiency and magnetic separability.

In search of better synthesis approaches, in recent years, further improvements have been made. Jamal *et al.* synthesized rGO@FeO@Fe_3O_4@TiO_2 nanocomposites[49] wherein rGO was prepared *via* modified Hummers' method by oxidizing graphite powder using sodium nitrate and potassium permanganate in sulphuric acid followed by reduction using ascorbic acid (Fig. 4). Iron species were incorporated using sodium borohydride reduction and TiO_2 was deposited through sol gel and hydrothermal treatment.

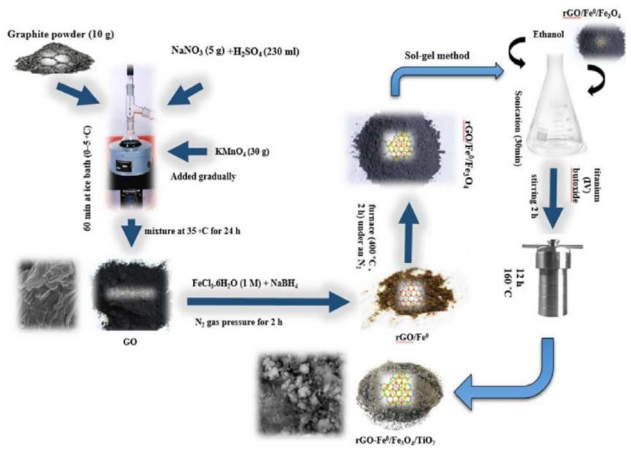

Fig. 4 Schematic representation of the synthesis of rGO, rGO@Fe^0, rGO@Fe^0@Fe_3O_4, and rGO@Fe^0@Fe_3O_4@TiO_2. Reproduced from ref. 48 with permission from Elsevier, copyright 2023.

Similarly, Bala *et al.* synthesized Cu_2O@CuO-decorated TiO_2@GO nanocomposites[50] *via* a liquid impregnation method, ensuring uniform copper dispersion. GO was synthesized by modified Hummers' method. The synthesis involves the treatment of TiO_2 with copper(II) nitrate, followed by calcination at 450 °C in argon and subsequent reduction at 280 °C in H_2 per argon. The resulting Cu_2O/CuO–TiO_2 was dried with GO in a ratio of 10 : 1. The content of copper was varied (1–3%) and all the variants resulted in a decreased PL (photoluminescence) intensity indicating effective charge carrier separation.

Gupta *et al.*[51] reported the synthesis of $CoFe_2O_4$@TiO_2/rGO nanocomposites. $CoFe_2O_4$ nanoparticles were prepared using a co-precipitation method followed by incorporation of pre-calcined TiO_2 under alkaline conditions at 90 °C. rGO was prepared using modified Hummers' method and the $CoFe_2O_4$@TiO_2/rGO composite was formed by addition of a stoichiometric ratio of $CoFe_2O_4$@TiO_2 into an ultrasonicated rGO suspension in water followed by refluxing the suspension at 95 °C for 2 h (Fig. 5).

3.3 MnO_2@Fe_3O_4@rGO and related nanocomposites

Manganese dioxide (MnO_2) has garnered significant research interest and attention owing to its unique physicochemical characteristics, and its extensive applications in supercapacitors,[52] batteries,[53] microwave absorption,[54] visible light-driven catalysis,[55] molecular sieves,[56] and water purification.[57]

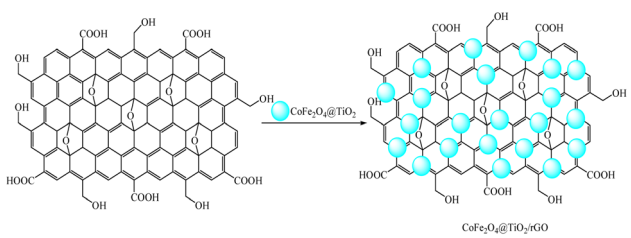

Fig. 5 rGO@TiO_2@$CoFe_2O_4$ nanocomposite synthesis.

Nevertheless, the structural instability, inadequate electroconductivity and difficulty in separation considerably limit its practical applications.[58] To enhance its performance further, it is essential to integrate other materials with MnO_2. The incorporation of Fe_3O_4 and GO@rGO can improve the properties of MnO_2, as Fe_3O_4 demonstrates commendable electronic conductivity.[59] Additionally, as part of a composite, Fe_3O_4 facilitates the recycling of multifunctional nanoparticles and enhances their stability.[55] GO@rGO provides an extremely large surface area, strong mechanical stability, and exceptional electrical conductivity.

The general scheme for the synthesis of MnO_2@Fe_3O_4@GO and MnO_2@Fe_3O_4@rGO nanocomposites as proposed by Yan Liu *et al.*[60] involves the preparation of GO by modified Hummers' method from natural flake like graphite. This is followed by the standard one-pot solvothermal method for the synthesis of Fe_3O_4@graphene oxide nanocomposite. Finally, MnO_2 is coated with Fe_3O_4@GO by simple immersion into $KMnO_4$ solution whose pH is controlled using HCl at 80 °C for 3 h. The research indicated that MnO_2@Fe_3O_4@GO exhibits a remarkable maximum adsorption capacity in both acidic and nearly neutral environments. The desorption results demonstrated that the adsorption capacity could persist at 76% after five cycles of use, suggesting that the MnO_2@Fe_3O_4@GO nanocomposite is a promising candidate for Cr(VI) adsorption.

A similar approach was used by Lichao Tan *et al.* in 2015 (ref. 61) and Jing Li *et al.* in 2017 (ref. 62) for the synthesis of MnO_2@Fe_3O_4@rGO nanocomposites. A three-dimensional (3D) hierarchical MnO_2 shell was observed, with an Fe_3O_4@MnO_2 core–shell structure coated by rGO layers. An examination of their electrical properties demonstrated that the effectiveness of the connection between Fe_3O_4@MnO_2 particles and graphene layers significantly affects the electrocapacitive performance of the Fe_3O_4@MnO_2@rGO composite.[60] Moreover, the MnO_2@-Fe_3O_4@rGO composite was found to be effective as an adsorbent for the sorption of uranium(VI).[61]

3.4 Synthesis of V_2O_5@Fe_3O_4@rGO and related nanocomposites

In recent decades, vanadium pentoxide (V_2O_5) has garnered significant interest among transition metal oxides due to its remarkable characteristics when combined with various supports for a range of applications.[63] V_2O_5 acts as a semiconductor metal oxide catalyst with a low band gap energy of 2.2 eV, which readily facilitates electron–hole recombination when exposed to light. Consequently, hybrid systems composed of V_2O_5 nanoparticles with reduced graphene oxide (rGO) sheets have demonstrated enhanced photocatalytic activity.[64] The incorporation of graphene sheets mitigates the premature recombination of electron–hole pairs, thus rendering them more accessible for photocatalytic processes. Additionally, Fe_3O_4 enhances conductivity and imparts magnetic properties, which contribute to its effective recovery.

Synthesis of an Fe_3O_4@V_2O_5@rGO nanocomposite by Purna K. Boruah *et al.*[65] describes an *ex situ* method where Fe_3O_4 NPs can be deposited on the surface of a V_2O_5@rGO nanocomposite

through chemical co-precipitation. The narrow band gap and distinct band gap energies of Fe_3O_4 and V_2O_5 demonstrated its suitability for visible light absorption.

Fatemeh Jafari *et al.*[66] proposed a different method for the synthesis of Fe_3O_4@V_2O_5@rGO nanocomposites involving the dissolution of Fe_3O_4@GO powder in ethylene glycol with a pH of 11–12 controlled using ammonia solution (25%). This is followed by the addition of NH_4VO_3, stirring and heating, autoclaving, washing, drying and finally annealing to form the composite. A similar strategy can be employed to synthesize Fe_3O_4@V_2O_5@GO nanocomposites. The results indicate that the graphene oxide substrate is effectively decorated using Fe_3O_4 and V_2O_5 nanoparticles and converted to reduced graphene oxide. Photoluminescence (PL) and diffuse reflectance spectroscopy (DRS) findings suggest that the incorporation of both V_2O_5 and Fe_3O_4 nanoparticles onto the reduced graphene oxide (rGO) nanosheets in the V_2O_5@Fe_3O_4@rGO composite significantly diminished the intensity and optical band gap energy, leading to enhanced charge transfer and reduced recombination of electron–hole pairs. The V_2O_5@Fe_3O_4@rGO composite demonstrates superior oxygen evolution activity, achieving an overpotential of 458 mV and a Tafel slope of 132 mV dec^{-1} in LSV, outperforming rGO, Fe_3O_4, V_2O_5, Fe_3O_4@rGO, and V_2O_5@rGO.

3.5 Synthesis of ZrO_2@Fe_3O_4@rGO and related nanocomposites

Zirconium oxide nanoparticles (ZrO_2 NPs) exhibit exceptional chemical and physical properties that render them highly versatile for various applications, such as fuel cells, gas sensors, optoelectronics, catalysts, and materials resistant to corrosion.[67–71] Owing to its large surface area and the presence of numerous oxygen vacancies, zirconium oxide is regarded as a promising candidate for photocatalytic applications within academic and scientific research.[72–75] As an adsorbent, zirconium enhances the adsorption process. The creation of ZrO_2 nanocomposites with Fe_3O_4 and GO/rGO results in improved characteristics and facilitates the recovery of the composite due to its magnetic properties.

In 2018, Nagi M. El-Shafai *et al.*[76] described a simple method for the synthesis of ZrO_2@Fe_3O_4@rGO in which GO sheets are dispersed in water and a solution containing $ZrOCl_2 \cdot 8H_2O$, $FeCl_2 \cdot H_2O$ and $FeCl_3 \cdot 6H_2O$ is added followed by addition of hot ethanolic KOH solution dropwise with continuous stirring. The reaction mixture is centrifuged, washed and vacuum dried to obtain the ZrO_2@Fe_3O_4@rGO nanocomposite. The synthesized GO-Fe_3O_4@ZrO_2 nanocomposite exhibited an energy band gap of 3.20 eV, as determined by optical absorption measurements, which was lower than that of GO and GO-Fe_3O_4. Additionally, the composite demonstrated enhanced adsorption capacity and photocatalytic activity.

A recent research study by Ali Fadhil Ismail *et al.*[77] showed that a ZrO_2@Fe_3O_4@rGO nanocomposite can be prepared by adding a calculated amount of ZrO_2 to aq. dispersion of Fe_3O_4@rGO and vigorously shaking the mixture for 1 h. This method can be used to synthesize ZrO_2@Fe_3O_4@rGO as well. Utilizing X-ray diffraction (XRD), field emission scanning electron microscopy (FESEM), and energy dispersive X-ray (EDX) analysis, it was confirmed that an amorphous phase was present, as evidenced by the strong peak positions at various lattice planes. The irregular shapes of the particles showed signs of aggregation.

3.6 Other significant contributions

In this section, synthesis of graphene oxide and Fe_3O_4 based nanocomposites which are less explored among the scientific community has been discussed. Cu based nanocomposites have been shown to be effective catalysts for the oxidation of *n*-hexane[78] and have also been employed in high performance super-capacitor applications.[79] They are also being studied for photo-catalytic effectiveness under visible light for the degradation of organic pollutants.[80–82] There are few reports in the literature regarding the synthesis of Cu-based magnetic metal oxide@GO nanocomposites which include CuO@Fe_3O_4@GO and CuS_2 @Fe_3O_4@GO nanocomposites. A general approach to synthesize such composites, as highlighted by Yachana Jain *et al.*[83] and Negin Nasseh *et al.*,[84] includes the synthesis of GO using Hummers' method followed by sonochemical attachment of Fe_3O_4 and CuS_2 or CuO nanoparticles on its surface (Fig. 6).

In the former, the M_s value of the synthesized nanocomposite was found to be lower than that of pure magnetite. Nevertheless, the magnetization remained sufficiently high, allowing for the effective removal of the catalyst from the reaction mixture. The XRD analysis of the synthesized catalyst revealed that the crystal structure of the Fe_3O_4 core remained unchanged during its immobilization on the surface of graphene oxide (GO). The absence of copper signals in the XRD pattern suggested that the Cu species are highly dispersed. Furthermore, no characteristic peaks of other impurities were identified. The composite demonstrated superior thermal stability compared to GO. TEM images clearly revealed that Fe_3O_4 and CuO nanoparticles had successfully integrated onto multilayer graphene oxide sheets. The synthesized catalyst exhibited remarkable catalytic activity and could be recycled up to 8 times. In the latter, the average size of CuS nanoparticles in the CS88F6G6 composite was reduced in comparison to its pure form. Additionally, the Fe_2O_3 nanoparticles possessed fine pores within their structure, which function as a template to inhibit the growth of CuS nanoparticles, thereby increasing the surface area for photocatalytic activity. The spherical CFS nanoparticles were unevenly dispersed on the surface of the smooth GO sheets. The CS88F6G6 nanocomposite exhibited

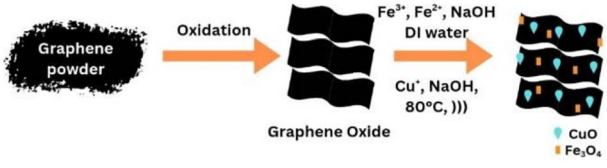

Fig. 6 Schematic representation of synthesis of GO-Fe_3O_4@CuO nanocomposites.

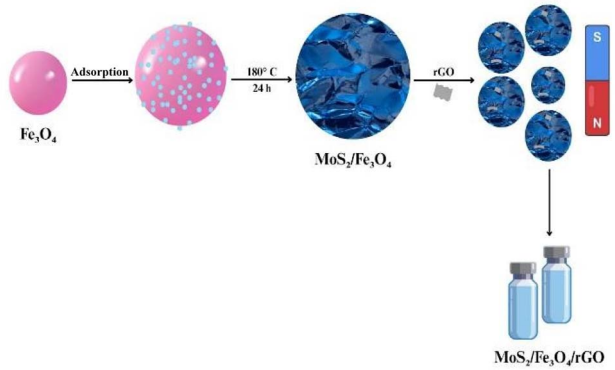

Fig. 7 Proposed mechanism for the formation of MoS_2@Fe_3O_4@rGO nanoparticles.

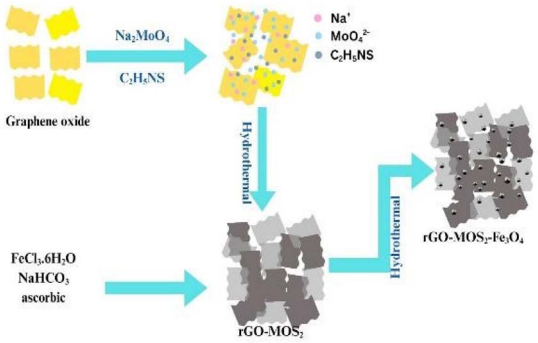

Fig. 8 Schematic illustration for the preparation of rGO-MoS_2-Fe_3O_4 nanocomposites.

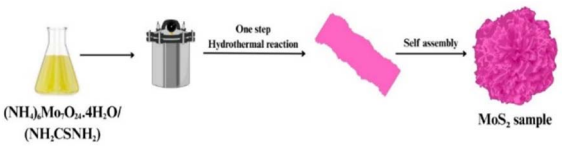

Fig. 9 The process of preparing MoS_2 by a one-step hydrothermal reaction.

superparamagnetic behaviour when subjected to an external magnetic field, allowing for easy recovery. Moreover, the nanocomposite showed strong absorption in the 400–700 nm range, making it highly suitable for visible-light-driven photocatalysis.

Molybdenum sulfide (MoS_2) is an n-type semiconductor[85] that has attracted considerable attention in the fields of photocatalysis,[86] sensors,[87] electrochemistry,[88] supercapacitors,[89] and drug delivery[90] owing to its natural abundance, well-developed crystalline structure, low production cost, favourable electrical conductivity, and large specific surface area. Moreover, the combination of MoS_2 with Fe_3O_4 and GO addresses the limitations of individual materials, such as the high density of Fe_3O_4,[91] issues with dispersion, and the tendency for two-dimensional GO and MoS_2 to stack, thereby enhancing wave absorption performance[92] and safeguarding magnetic metals.[93] Many research studies have focused on the synthesis of MoS_2@Fe_3O_4 @rGO with only the recent studies paving the pathway for the direct synthesis of Fe_3O_4@-rGO@MoS_2 and Fe_3O_4@rGO@Ag@MoS_2 nanocomposites (Fig. 7).

In 2018, Dongzhao Mu *et al.*[94] synthesized MoS_2@Fe_3O_4@-rGO nanocomposites using a simple procedure by dispersing monodispersed Fe_3O_4 nanoparticles in distilled water under ultrasonic radiation followed by the slow addition of Na_2MoO_4 and L-cysteine under mechanical stirring at room temperature.

This was followed by the dropwise addition of a GO suspension with continuous stirring and then autoclaving the reaction mixture at 180 °C for 24 h. The physicochemical properties of the prepared nanocomposite are displayed in Table 1.

A similar procedure was followed by Somayeh Tajik *et al.*[95] for the synthesis of MoS_2@Fe_3O_4@rGO nanocomposites (Fig. 8 and 9).

A different two-step hydrothermal method was proposed by Xiao Ding *et al.*[96] for the preparation of rGO-MoS_2 composites:

The preparation included the synthesis of GO nanoparticles using the modified Hummers' method followed by ultrasonic dispersion and slow addition of aq. sodium molybdate and thioacetamide, autoclaving the mixture at 220 °C for 24 h and separating the product through centrifugation. The second step included the dispersion of $FeCl_3 \cdot 6H_2O$, $NaHCO_3$, ascorbic acid and rGO@MoS_2 composite in water through ultra-sonication followed by autoclaving at 180 °C for 18 h. The MoS_2@Fe_3-O_4@rGO composite was obtained by cooling, washing and then freeze-drying the precipitate overnight. The synthesized nanocomposite featured a three-dimensional architectural structure and demonstrated remarkable microwave absorption capabilities despite its minimal thickness. The lowest reflection loss (RL) recorded was 47.67 dB at a frequency of 17.44 GHz with a thickness of 1.5 mm. Additionally, the maximum effective absorption bandwidth (RL B10 dB) achieved was 4.72 GHz when the thickness was increased to 1.7 mm.

Zhenjun Wang[97] synthesized 3D flower-like MoS_2@Fe_3O_4@-rGO composites using a three-step process involving the

Table 1 The corresponding physicochemical properties of MoS_2, MoS_2@Fe_3O_4 and MoS_2@Fe_3O_4@rGO[94]

Sample	Average crystal size [nm] (standard deviation)	S_{BET} [m^2 g^{-1}]	Pore volume [cm^3 g^{-1}]
MoS_2	18.22	8.16	0.04
MoS_2@Fe_3O_4	21.32	22.59	0.12
MoS_2@Fe_3O_4@ rGO	10.27	72.23	0.185

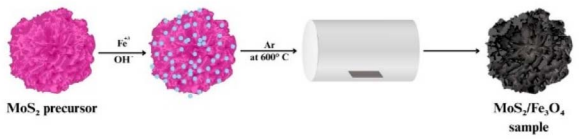

Fig. 10 The preparation process of MoS_2@Fe_3O_4 composites.

synthesis of MoS_2 through a one-step hydrothermal method, followed by preparation of MoS_2@Fe_3O_4 as shown in Fig. 10.

This was followed by the preparation of MoS_2@Fe_3O_4@rGO *via* ultrasonic dispersion of GO/EG solution and MoS_2@Fe_3O_4@EG (ethylene glycol) solution, resulting in a GO@MoS_2@Fe_3O_4 suspension. The final composite was then obtained through a solvothermal process (Fig. 10). The core–shell composite MoS_2@Fe_3O_4@rGO demonstrated a minimum reflection loss (RL) of −64.05 dB at a frequency of 1.83 mm, along with an effective absorption bandwidth (RL < −10 dB) of 7.34 GHz at 2.5 mm (spanning from 10.66 to 18 GHz), which was significantly greater than that of pure MoS_2 and MoS_2@Fe_3O_4 microspheres.

Latest research by Shilpa R. Amonkar and Sudhir Cherukulappurath[98] shows that MoS_2@Fe_3O_4@GO nanocomposites can be easily synthesized using the following approach. In addition to this Fe_3O_4@GO@Ag@MoS_2 can also be synthesized using the same procedure by employing Fe_3O_4@GO@Ag as a substrate. The SEM image of Fe_3O_4@MoS_2 demonstrated that the hybrid composite is composed of both Fe_3O_4 nanoparticle clusters and flower-like MoS_2 microspheres. It was noted that the Fe_3O_4 clusters were enveloped by the flower-like MoS_2 microspheres (Fig. 11).

As evident from the above discussions, to summarize, the synthesis of magnetically retrievable metal oxide@graphene oxide nanocomposites involves the preparation of three different components – the magnetic material, the metal oxide and Graphene Oxide (GO) – and their integration to produce the nanocomposites.

The nanoparticles of various magnetic materials such as Fe_3O_4, $CoFe_2O_4$, and $CuFe_2O_4$ are prepared using common methods of nanoparticle synthesis including hydrothermal, solvothermal, co-precipitation and sol–gel methods.

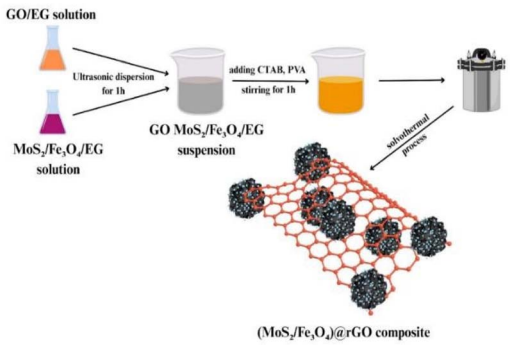

Fig. 11 Synthesis of porous MoS_2@Fe_3O_4@rGO composites.

Photocatalytic metal oxides such as ZnO, TiO_2, and CuO are synthesized using hydro- or solvothermal methods, while GO is synthesized using the Hummers or modified Hummers' method. The most commonly used method for the synthesis of nanocomposites first involves the preparation of a GO/magnetic material composite, followed by the dispersion of the synthesized metal oxide.[99] However, other methods of synthesis have also been developed by altering the order in which the different components are introduced and through the *in situ* synthesis of nanoparticles in the reaction medium.[100]

4. Photocatalytic degradation of wastewater pollutants

This section explains the role of magnetic metal oxide@graphene oxide based nanocomposites in photocatalytic degradation of organic pollutants generally found in wastewater.

4.1 Pharmaceuticals

Pharmaceuticals represent a category of both synthetic and natural chemicals that possess bioactive properties, specifically formulated and produced to provide therapeutic benefits against illnesses or to prevent the onset and transmission of diseases in humans and animals. These substances can be found in the form of over-the-counter medications, prescription drugs, or veterinary treatments.[101] The increasing prevalence of these compounds is observed yearly around the globe, driven by the emergence of new illnesses and the introduction of novel pharmaceuticals aimed at treating these conditions. Recent data from IQVIA reveal that the worldwide consumption of medicines has surged by 14% over the last five years and is anticipated to rise by an additional 12% by 2028, reaching an annual total of 3.8 trillion defined daily doses.[102] However, the extensive use of pharmaceuticals in everyday life has led to the emergence of contaminants, potentially harming both human health and aquatic ecosystems.[103–105] Globally over 3000 chemical substances, with concentrations varying from ng L^{-1} to μg L^{-1}, including pharmaceuticals, have been detected in wastewater, surface water, soil, groundwater, and drinking water.[106–108] Pharmaceutical compounds can enter the environment through direct discharges from drug manufacturing, excretion by patients and animals, aquaculture, and the inappropriate disposal of unused or expired medications, resulting in environmental contamination (UNEP).

The existence of these pharmaceutical pollutants poses serious risks, including cancers, organ damage, congenital abnormalities, reproductive issues, endocrine disturbances, and a range of toxic effects, from mild to severe, in the global population. The toxic effects of these chemicals have also been observed in mammals and other living beings and the overall ecosystem.[109] Furthermore, antibiotic-resistant bacteria can emerge and antibiotic-resistant genes may spread among humans and other organisms due to the accumulation of antibiotic medications in water sources.[110]

Heterogeneous photocatalysis has been shown by many studies to be an efficient, eco-friendly and economical method for the degradation of pharmaceutical contaminants.[111,112] The various magnetic metal oxide@GO photocatalytic agents that have been reported for the breakdown of different types of pharmaceutical agents have been covered in the following subsections.

4.1.1 Antimicrobials. Antimicrobials are chemotherapeutic substances that encompass a widely utilized category of agents, including antibiotics, antivirals, antifungals, and antiparasitics, aimed at preventing and treating infections in humans, aquaculture, livestock, and crops due to various pathogenic bacteria, viruses, fungi, and more. They were designed to reduce mortality rates and enhance the immune response in both humans and animals. However, only 30% of the developed antibiotics are currently employed in combating diseases, while the remaining 70% are improperly released into the environment without undergoing metabolism. The majority of these antimicrobials in the environment are poorly metabolised which allows them to persist there and lets them enter the food chain. These are ingested by both humans and animals; consequently, it facilitates the emergence and spread of antibiotic-resistant bacteria and antibiotic resistance genes.[104,113] Thus, there has been a primary focus on their removal from aqueous environments through a photocatalytic approach.

A magnetically recyclable $CuFe_2O_4$@rGO nanocomposite with varying concentrations of graphene oxide was synthesized using the hydrothermal method by Aruljothi *et al.*,[114] and the photocatalytic performance of this nanocomposite was evaluated under sunlight exposure (Fig. 12). The experimental findings indicated that the $CuFe_2O_4$@rGO (10 wt%) nanocomposite exhibited the highest photocatalytic efficiency in degrading tetracycline.

In 2016, Disi Qiao *et al.*[115] reported the photocatalytic degradation of tetracycline using an Fe_3O_4@GO@ZnO magnetic nanocomposite, where graphene oxide served as the framework to enhance electron transfer and ZnO functioned as an effective photocatalyst, achieving a 74% degradation of tetracycline hydrochloride under visible light irradiation within 100 min. The catalyst was found to be effective up to four cycles of use. A more efficient magnetic nanocomposite, C_3N_4@MnO_2@GO, synthesized by Chunyan Du *et al.*[116] in 2021, demonstrated an improved ability to photodegrade tetracycline hydrochloride under visible light, reaching a degradation rate of 91.4% in just 90 min.

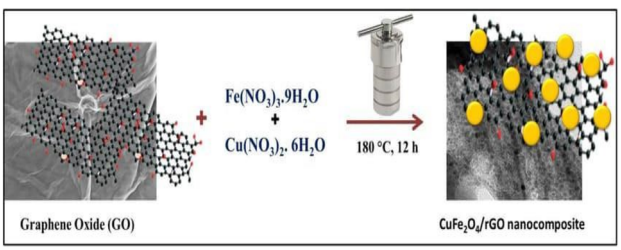

Fig. 12 Schematic diagram showing the synthesis of a $CuFe_2O_4$@rGO nanocatalyst. Reproduced from ref. 114 with permission from John Wiley and Sons, copyright 2023.

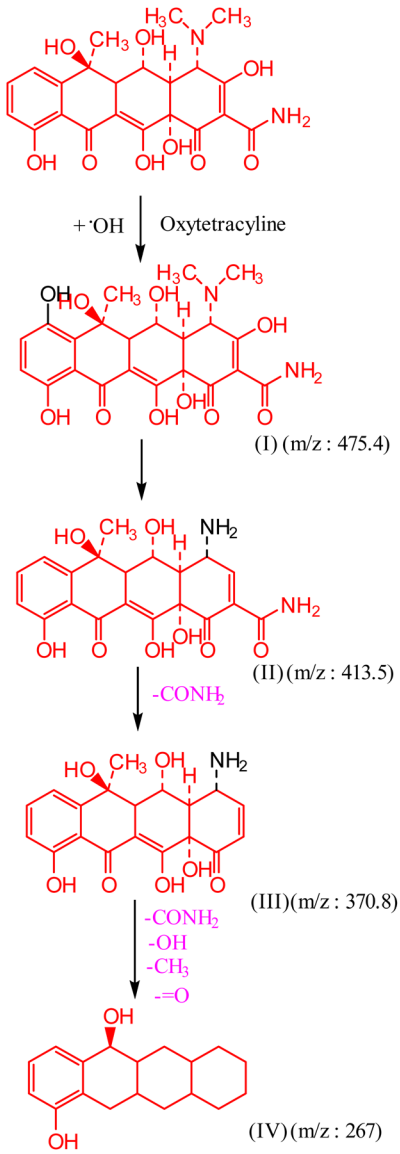

Fig. 13 Diagrammatic representation of the proposed mechanism for the degradation of oxytetracycline under solar irradiation using a Co_3O_4@TiO_2@GO photocatalyst.

Shi *et al.*[117] demonstrated the photo-Fenton degradation of tetracycline (TC) using a CdS@reduced graphene (rGO)@$ZnFe_2O_4$ (ZFO) nanocomposite system under visible light exposure; a TC removal of 80% and 59.2% mineralization can be achieved.

The Co_3O_4@TiO_2 graphene oxide nanocomposite synthesized by Jo *et al.*[118] through sol–gel and hydrothermal methods exhibited an excellent performance for the photocatalytic degradation of oxytetracycline under solar and visible light, achieving 91% efficiency in 90 min attributed to improved photoinduced charge separation and associated hydroxyl radical formation (Fig. 13).

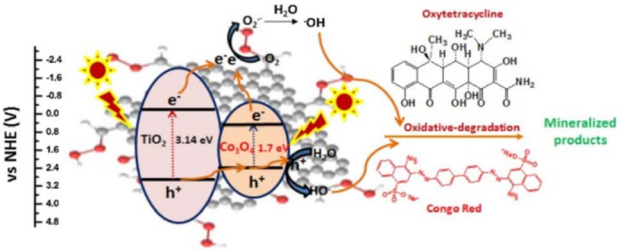

Fig. 14 Schematic diagram of photocatalytic degradation of oxytetracycline and Congo red under solar irradiation. Reproduced from ref. 119 with permission from Elsevier, copyright 2017.

Recently, a novel photocatalyst composed of magnetic porous cobalt ferrite@rGO (CF@rGO) balls has been synthesized by Wang *et.al.* using a modified microfluidic method (Fig. 14). The resulting photocatalyst (CF@rGO) exhibited remarkable stability in cyclic experiments with great magnetic separability and has been effectively used for the photodegradation of oxytetracycline achieving a degradation efficiency of 84.7%.[119]

Numerous studies have shown that graphene oxide magnetite (GO@Fe_3O_4) works as an effective photocatalyst for the degradation of ciprofloxacin in water using visible light, achieving efficiencies between 80 and 90% under optimal conditions of pH and MO@GO concentration.[120,121] The photocatalytic properties of this catalyst can be further improved by incorporating TiO_2 nanoparticles, as illustrated in the research conducted by Uruș *et al.*,[122] where the GO@Fe_3O_4@TiO_2 nanocomposite was synthesized using an *in situ* method that successfully removed 91.5% of ciprofloxacin from water in 240 min.

A similar study conducted by Farhadian *et al.*[123] utilized a TiO_2@Fe_2O_3@GO nanocomposite for the degradation of metronidazole under aqueous conditions under UV light irradiation. Under optimal conditions of 10 mg L^{-1} metronidazole concentration, a photocatalyst concentration of 1 g L^{-1}, an irradiation time of 120 min and a pH of 5 an efficiency of 97% is achieved.

Focusing on the degradation of norfloxacin with activated peroxodisulfate (Fig. 15), Wu *et al.*[124] investigated a UV-assisted nitrogen-doped reduced graphene oxide@Fe_3O_4 composite created through a simple hydrothermal-co-precipitation method. At a pH of 3.0, 100% degradation of norfloxacin was achieved within 13 min.

Working on a similar line, Kakavandi *et al.*[125] developed a ternary nanocomposite by integrating TiO_2 nanoparticles with a magnetic core–shell structure onto rGO to form Fe_3O_4@SiO_2@TiO_2@rGO (FST@rGO). This photocatalyst was then used to degrade the metronidazole (MNZ) antibiotic through the photocatalytic activation of peroxydisulphate (PDS) in a batch environment. The results showed the remarkable effectiveness of FST@rGO in the photodegradation of metronidazole across a wide range of pH. Under ideal conditions (pH: 7, PDS: 3 nM and FST@rGO: 0.1g L^{-1}), over 94% of MNZ and 58% of total organic carbon were removed within 60 minutes of exposure to UV light (Fig. 16).

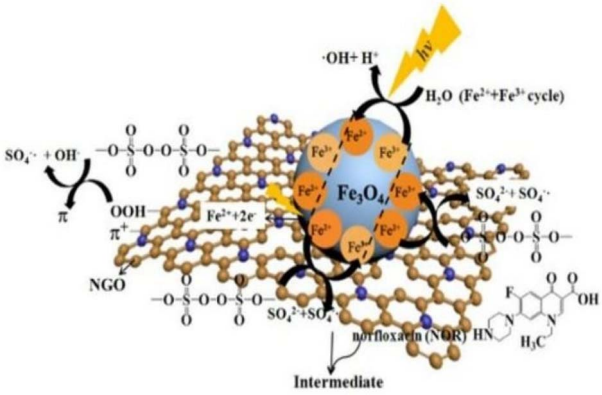

Fig. 15 Schematic representation of the photocatalytic degradation of norfloxacin using a nitrogen-doped reduced graphene oxide@Fe_3O_4 nanocomposite. Reproduced from ref. 124 with permission from Taylor & Francis, copyright 2020.

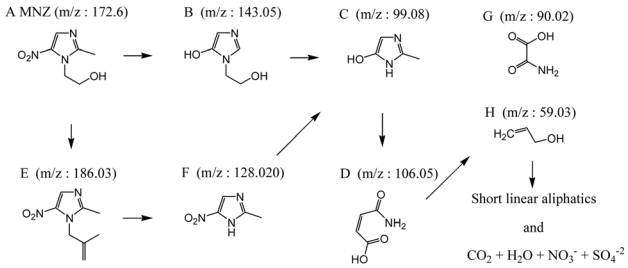

Fig. 16 The proposed reaction mechanism for the degradation of metronidazole.

Wan *et al.*[126] showed that Fe_3O_4@Mn_3O_4-rGO NCs serve as an effective photocatalyst for the degradation of sulfamethazine in an aqueous solution (Fig. 17). Under optimal conditions of 0.5 g L^{-1} photocatalyst concentration, 0.07 mm L^{-1} sulfamethazine at pH 3, a temperature of 35 °C, and 6 mm L^{-1} concentration of H_2O_2 a photodegradation efficiency of 98% for sulfamethazine was observed. A novel photocatalyst, ZnO@Fe_3O_4-GO@ZIF, combining the features of magnetic graphene oxide and metal–organic frameworks synthesized by Chen *et al.*,[127] exhibited rapid degradation of three antibiotics—metronidazole, sulfamethazine, and norfloxacin—under simulated solar radiation

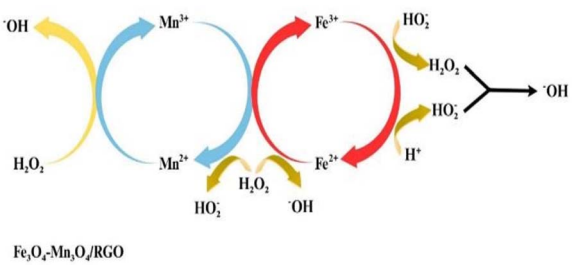

Fig. 17 Diagrammatic representation of the ROS formed during the photocatalytic degradation of sulfamethazine using an Fe_3O_4@Mn_3O_4rGO nanocomposite.

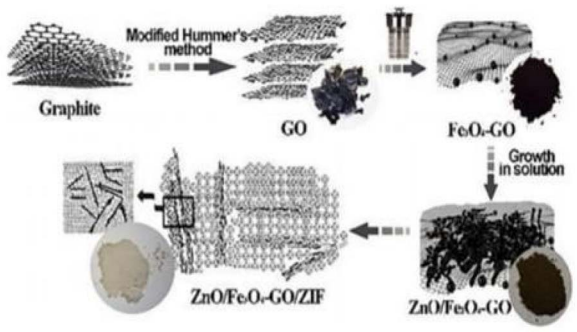

Fig. 18 Synthesis of a ZnO@Fe_3O_4-GO@ZIF nanocomposite. Reproduced from ref. 127 with permission from Springer Nature, copyright 2021.

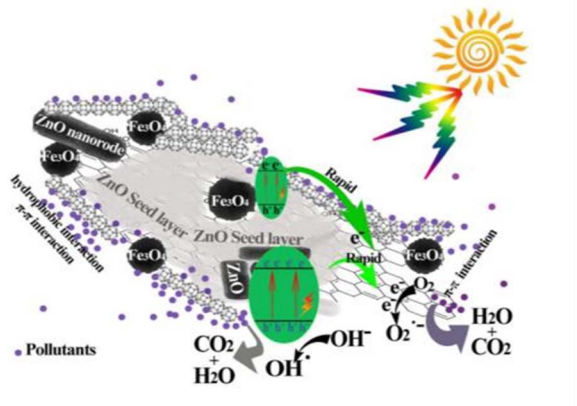

Fig. 19 Diagrammatic representation of the proposed mechanism for photocatalytic degradation of metronidazole, sulfamethazine and norfloxacin. Reproduced from ref. 127 with permission from Springer Nature, copyright 2021.

for 1 h (Fig. 18 and 19). This resulting photocatalyst could be recycled at least ten times without significant deactivation.

A slightly different approach was employed by Nimshi *et al.*[128] through a sonophotocatalytic degradation process. They synthesized $CoFe_2O_4$@TiO_2@rGO (CoTG) ternary nanocomposites *via* cost effective and environment-friendly green microwave and sol–gel methods. Pedalium murex plant's leaf extract served as the reducing and stabilizing agent during the microwave synthesis. Its sonophotocatalytic degradation capabilities were examined against tetracycline and ciprofloxacin antibiotics in the presence of ultrasonic irradiation and visible light. Impressive efficiencies of 92% and 84% for the degradation of tetracycline (20 mg L^{-1}) and ciprofloxacin (10 mg L^{-1}) in a short timeframe were demonstrated.

A magnetically separable core–shell heterostructured photocatalyst Fe_3O_4@Bi_2O_3@RGO was successfully synthesized for the first time through a self-assembly method by Zhu *et al.*[129] In the degradation of quinolone antibiotics (QAs) under visible light irradiation, the synthesized Fe_3O_4@Bi_2O_3@RGO nanocomposites displayed an expanded range of visible light absorption, enhanced efficiency in charge separation, and excellent photocatalytic performance and cycling stability. The degradation rate of ciprofloxacin (CIP) using this photocatalyst reached an impressive 98.3% within 240 min, remaining above 80% even after ten photocatalytic reaction cycles.

Mehralipour *et al.*[49] synthesized an rGO@Fe^0@Fe_3O_4@TiO_2 nanocomposite *via* Hummers' method and a straightforward sol–gel approach to study photocatalytic degradation of penicillin G in aqueous media (Fig. 19). Using central composite design, nanocomposite dosage (10–20 mg L^{-1}), pH (4–8), penicillin G concentration (50–100 mg L^{-1}) and reaction time (30–60 min) were optimized and an efficacy of 96% was achieved at catalyst dose = 18.5 mg L^{-1}, pH = 6.5, penicillin G concentration = 52 mg L^{-1} and reaction time = 59.1 min. Besides being magnetically retrievable the catalyst displayed high recyclability up to 5 cycles.

In a separate investigation, the engineered rGO@α-γ-Fe_2O_3 exhibited remarkable photodegradation efficiency for the antibiotic rifampicin, achieving a degradation rate of 82.1% within 80 min of light exposure, utilizing 0.2 mg mL^{-1} of the rGO@α-γ-Fe_2O_3 based photocatalyst[130] (Fig. 20).

4.1.2 Antipyretics. Antipyretics are compounds which are used to alleviate fever.[131,132] They have become emerging environmental pollutants, largely due to their extensive use and subsequent discharge into wastewater. In particular, acetaminophen (paracetamol) poses a significant threat due to its widespread use and discharge into water bodies. It has been detected in wastewater, surface waters and drinking water and *via* oxidative conversion it is converted into *N*-acetyl-*p*-benzoquinone imine which results in toxicity. The stable chemical structure of acetaminophen is a major obstacle to its elimination through standard wastewater treatment techniques. The high solubility of antipyretics contributes to their widespread occurrence in wastewater treatment facilities, where they can endanger both the environment and public health.[133–135] As a result, there is an increasing emphasis on eliminating them from water through photocatalysis.

Despite limited research on the degradation of antipyretic medications utilizing magnetic graphene oxide-based nanocomposites, the investigation conducted by Chen *et al.*[127] highlighted the remarkable degradation of acetaminophen (paracetamol) using the ZnO@Fe_3O_4-GO@IF nanocomposite under solar irradiation for 1 h.

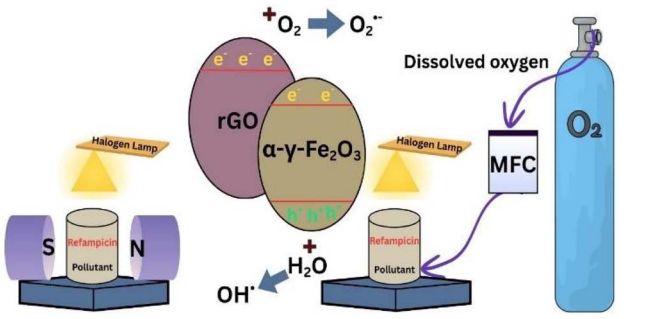

Fig. 20 Schematic representation of the removal of rifampicin using rGO@α-γ-Fe_2O_3 assisted by an external magnetic field and dissolved oxygen.

By a similar approach, Santosh Kumar *et al.*[136] using the chemical reflux method developed iron oxide nanorods uniformly coated on polypyrrole/reduced graphene oxide (Fe_3O_4@PPy@rGO) nanohybrids. Photocatalytic studies under visible light indicated that the Fe_3O_4@PPy@rGO nanohybrids in the presence of persulfate achieved an 84% degradation of acetaminophen (ACP).

4.1.3 Psychopharmaceuticals. Psychopharmaceuticals are drugs that exert therapeutic effects on the central nervous system influencing the pathological changes in experiences and behaviours associated with mental health conditions. They include five basic categories: antipsychotics, antidepressants, stimulants, mood stabilizers, and anxiolytics.[137] Psychopharmaceuticals and related illicit substances designed to interact with the human nervous system may also have the potential to affect the nervous systems of non-target organisms, potentially leading to adverse ecological consequences that alter their physiology and behaviour. Therefore, their removal from aquatic environments is crucial.[138,139] The photocatalytic degradation of these substances using magnetic graphene oxide-based nanocomposites is illustrated in this section.

A magnetically recyclable GO-TiO_2 composite, as reported by Linley *et al.* in 2014 (ref. 140), within 60 min under UV irradiation achieved up to 99% removal of carbamazepine and caffeine from aqueous solutions. This composite demonstrated superior photocatalytic activity compared to commercial P25, while also offering the benefits of high recoverability and reusability.

The graphene oxide-based magnetic photocatalyst Fe_3O_4@GO, as proposed by da Silva *et al.*,[141] exhibited exceptional efficiency in treating water contaminated with clonazepam through photo-Fenton degradation (Fig. 21 and 22).

The rGO-loaded-magnetite composites synthesized by Moztahida *et al.*[142] using a cost-effective co-precipitation method demonstrated remarkable efficiency in the photodegradation of carbamazepine. The hybrid composite highlighted a high photodegradation ability of 98.7% within 3 h at a pH of 6.5 (Fig. 23–25).

4.1.4 Estrogens. Estrogens are the primary female sex hormones, responsible for regulating the development of secondary sexual characteristics and the female reproductive system. They can be used therapeutically for treating different endocrine related disorders. However, their inappropriate use and release into the environment can lead to pollution. Estrone (E1), 17β-estradiol (E2), estriol (E3), and 17-α ethynyl estradiol (EE2) are some of the examples of estrogens that pose substantial environmental hazards.[143] These estrogens are found in trace amounts in the environment, such as in soil, surface water, or seawater, and have been associated with breast

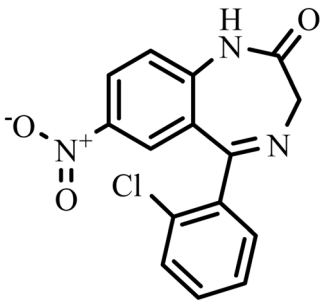

Fig. 22 Molecular structure of clonazepam.

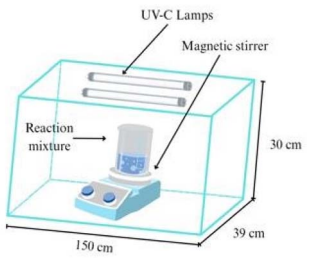

Fig. 21 Diagrammatic representation of the photoreactor.[141]

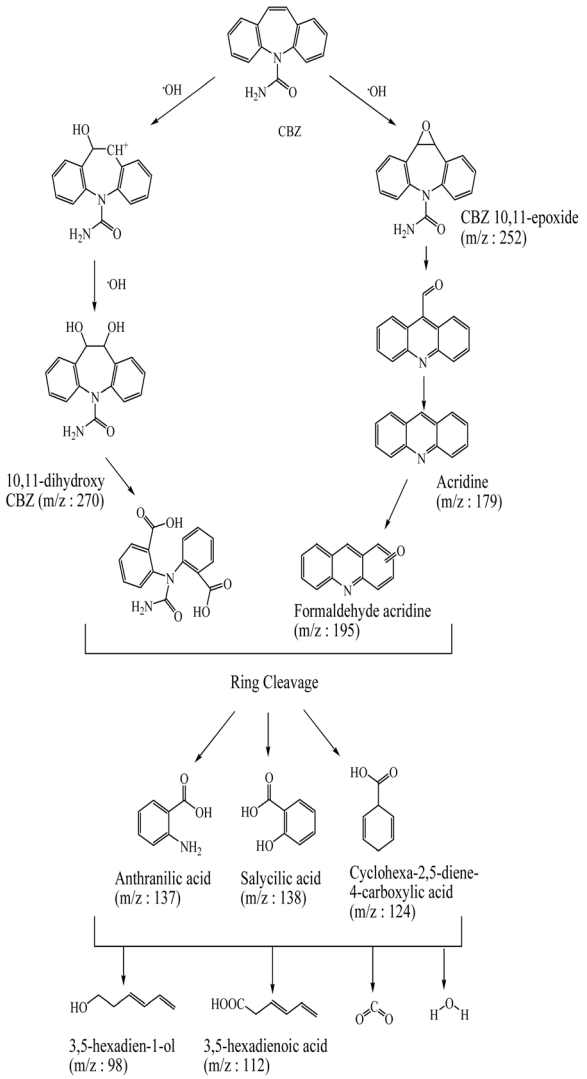

Fig. 23 Pathway of carbamazepine degradation and the intermediates formed.

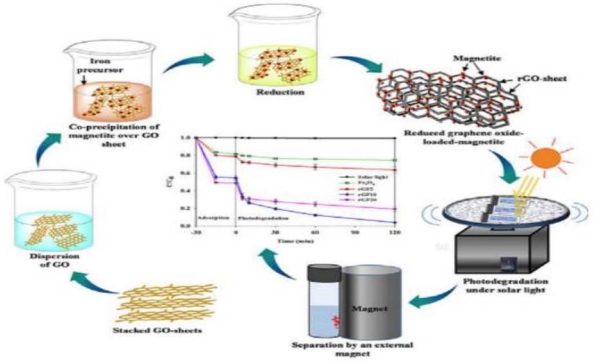

Fig. 24 Schematic representation of the process of synthesis of rGO loaded-magnetite, its role as a photocatalyst in the degradation of carbamazepine and its separation using an external magnet. Reproduced from ref. 142 with permission from Elsevier, copyright 2019.

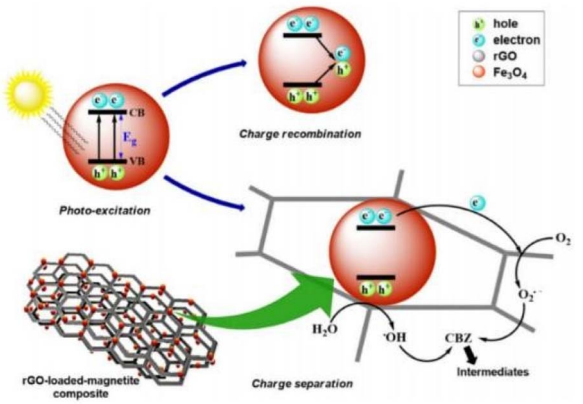

Fig. 25 Proposed mechanism for the production of ROS during the photocatalytic degradation of carbamazepine. Reproduced from ref. 142 with permission from Elsevier, copyright 2019.

cancer, ovarian cancer, fish feminization, low sperm count in adult males, endometriosis, obesity, cardiovascular endocrinology, and fibroids.[144,145] This highlights the importance of successfully removing them from the environment.

According to a research study by Ajibola A. Bayode *et al.*[146] the steroid hormones estrone, 17β-estradiol, estriol, and ethinyl estradiol were successfully oxidized and mineralized using a photocatalytic nanocomposite composed of kaolinite, pulverized *Carica papaya* seeds, 3-aminopropyltriethoxysilane (APTES), hematite (Fe_2O_3), and graphene oxide (GO). Even when all estrogens were present in the same water sample, the use of this photocatalytic nanocomposite still resulted in more than 80% steroid estrogen oxidation (Fig. 26).

Reusable, magnetically separable $ZnFe_2O_4$-Ag/rGO nanocomposites (NCs) were synthesized by Khadgi *et al.*[147] by co-modifying $ZnFe_2O_4$ with GO and Ag nanoparticles (NPs) through a simple one-pot hydrothermal method. Under visible light the photocatalytic performance of the catalyst was evaluated for successful degradation of 17α-ethinylestradiol (EE2). Under visible light irradiation 80% degradation of 17α-

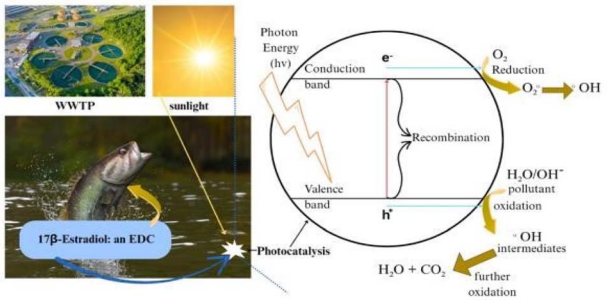

Fig. 26 Schematic illustration depicting the photodegradation of harmful estrogen present in aqueous media.

ethinylestradiol was achieved. Reusability up to 5 cycles showed a decline in photocatalytic activity from 100 to 70%.

4.1.5 Antidiabetic drugs. Antidiabetic drugs are those which are used in the management of diabetes or high blood glucose levels in the body. With the increase in the prevalence of diabetes in the past few decades the demand for these drugs has increased dramatically. For type II diabetes mellitus, metformin (Met) has proven to be a convenient and effective pharmaceutical treatment. Unlike plenty of other pharmaceutical drugs, it is not metabolised by humans; rather it passes through the body unaltered and enters aquatic compartments such as in sewage.[148] But by conventional wastewater treatment, these drugs are not effectively removed and end up in surface, ground and even drinking water. This poses potential risks to aquatic ecosystems and potentially to human health.[149,150] The degradation of metformin *via* magnetic metal oxide/graphene oxide-based nanocomposites holds good promise in its removal from the environment.

Khavar *et al.*[151] synthesized a novel hybrid nanostructured spherical catalyst, Fe_3O_4@rGO@ZnO/Ag-NPs (FGZAg), which under both ultraviolet and visible light irradiation effectively degraded metformin (MTF) (Fig. 27). The fabrication of the catalyst employed Fe_3O_4 microspheres as templates, which were coated with GO and ZnO shells, followed by decoration with Ag nanoparticles (NPs), and finally annealed in a nitrogen atmosphere. FGZAg achieved 60% mineralization and complete degradation of 20 mg L^{-1} MTF within 60 minutes in the visible-light photocatalytic process.

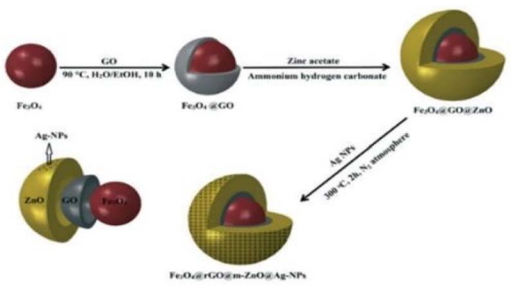

Fig. 27 Schematic representation of the synthesis of onion-like Fe_3O_4@rGO@ZnO@Ag nanoparticles. Reproduced from ref. 151 with permission from the Royal Society of Chemistry, copyright 2019.

4.2 Microplastics

Microplastics are defined as any particles made of plastic with a size smaller than 5 mm.[152] They can be broadly divided into two categories based on their origin: primary and secondary microplastics. Primary microplastics are those that are manufactured and intentionally added to consumer and commercial products such as cosmetics, personal care items, pharmaceuticals, detergents, and insecticides. In contrast, secondary microplastics are the ones that arise unintentionally from the degradation of larger plastic materials through various physical, chemical, or biological processes, including items like plastic bottles, plastic bags, and food containers and fishing gear made from plastic.[153,154] It is estimated that about 10 million tons of plastic waste enter the ocean annually (UNESCO) from various sources, with wastewater treatment plants (WWTPs), surface runoff from contaminated areas or disposal sites, and littering on beaches as the primary contributors.[155] The most widely used plastics globally include polyethylene (PE), low-density polyethylene (LDPE), high-density polyethylene (HDPE), polypropylene (PP), polystyrene (PS), polyvinyl chloride (PVC), and polyurethane, with many of these polymeric materials being difficult to recycle.[156]

The presence of microplastics in the environment poses a considerable threat to various living organisms, including microorganisms, humans, animals, and plants. Within the environment, microplastics disrupt both terrestrial and aquatic ecosystems.[157–162] In marine settings, they are consumed by a large number of diverse species. Microplastics can block the digestive tract, diminish food intake, harm the intestines, and trigger oxidative stress, resulting in internal injuries, decreased nutrient absorption, and potentially death. Additionally, microplastics can inhibit plant and algae growth, photosynthesis, and gene expression.[157–159] In soil, microplastics can modify water retention, alter the soil structure, and negatively impact beneficial microorganisms, thereby reducing agricultural productivity and food security.[159]

Microplastics have also been detected in various tissues of both animals and humans, including blood, brain, placenta, and reproductive organs.[160,161] They have even been identified in breast milk. In humans and animals, microplastics can lead to inflammation, oxidative stress, and disruption of the gut microbiome, which may result in gastrointestinal problems, liver damage, and potential endocrine and reproductive disorders[160–162] Moreover, they can transport persistent toxic substances such as phthalates and bisphenol A, which may lead to further complications.[160–163] Thus, there is an urgent need to remove these contemporary pollutants from the environment.

The removal of microplastics from water or wastewater involves challenges due to their inherent physical and chemical properties.[164] Microplastics can be degraded using several techniques, including biodegradation, chemical processes, and thermal treatment. While these methods may be effective for removing microplastics from water, they often require considerable time and financial investment and involve high energy demands.[165–167] Recently, the mineralization of microplastics through photodegradation has attracted significant attention among the scientific community, as it converts contaminants into non-hazardous compounds in a quick, effective, and cost-efficient manner.

Researchers have utilized TiO_2-based nanomaterials, TiO_2-rGO and titanium dioxide (TiO_2)/gold nanorods (AuNRs)@rGO, for the efficient degradation of polypropylene and polystyrene through photocatalysis for environmental pollution mitigation.[168,169]

In another study, an In_2O_3-rGO nanocomposite-based metal oxide exhibited efficient photocatalytic degradation of polyethylene films when exposed to visible light for varying durations of 0, 10, 20, 30, 40, and 50 h. A degradation efficiency of 99.47% was achieved in 50 h, as confirmed by thermogravimetric analysis.[170]

A recent study by Uogintė *et al.* highlights the application of graphene oxide-based metal oxide nanomaterials for the effective removal of polyethylene microplastic particles through photocatalytic degradation[171]

The use of magnetic metal oxide@graphene oxide in photocatalytic degradation of microplastics has been introduced quite recently which requires further investigation for its practical implementation. Nevertheless, there are numerous studies reported in the literature that show great potential for its application. For instance, TiO_2 and ZnO nanoparticles, along with their nanocomposites comprising pure metals, metal sulfides, C and N dopants, heterojunctions, and organic frameworks, have been demonstrated to exhibit remarkable efficiency under optimal conditions of irradiation, pH, and concentration in degrading polythene (PE), polypropylene (PP), polystyrene (PS), polyethylene terephthalate (PET), and polyvinyl chloride (PVC) (Fig. 28–30). In addition to TiO_2 and ZnO, other photocatalysts like CeO_2, Fe_2O_3, and CuO@$BiVO_4$ have also been found effective for degrading microplastics from water samples.[168,172,173]

Therefore, the findings reported in the existing literature support the concept of utilizing magnetic metal oxide@graphene oxide-based nanocomposites for the elimination of microplastics from water, with the added benefits of easier

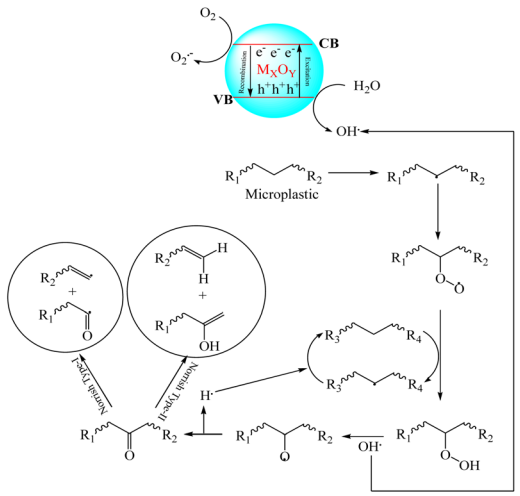

Fig. 28 Photocatalytic mechanism for microplastic degradation under light irradiation using metal oxide semiconductors.

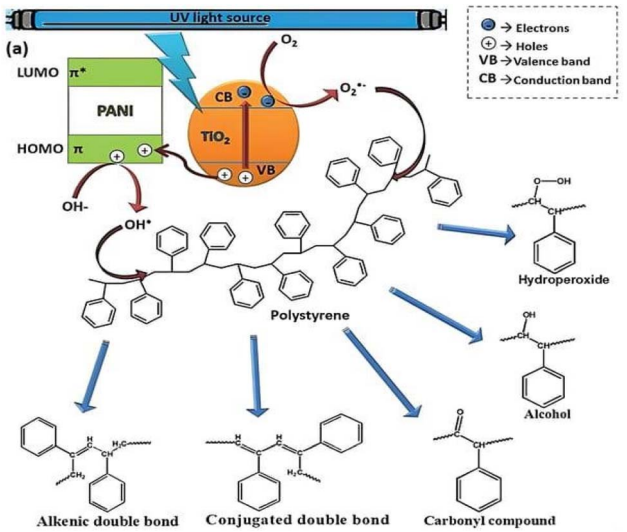

Fig. 29 Schematic diagram of the proposed mechanism for polystyrene photodegradation using TiO_2-PANI nanocomposites as a catalyst. Reproduced from ref. 172 with permission from John Wiley and Sons, copyright 2023.

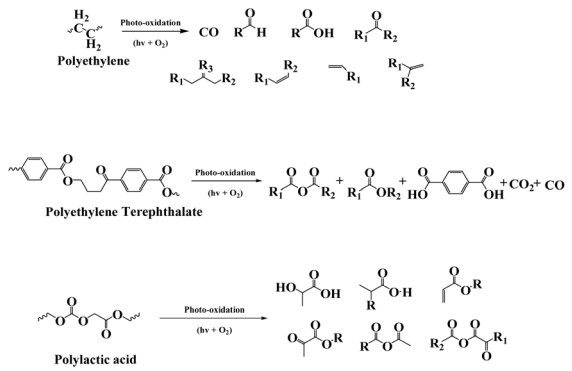

Fig. 30 Photocatalytic degradation mechanisms of polyethylene, polyethylene terephthalate and polylactic acid.

recovery, enhanced efficiency and reusability, thus making this a promising area of research.

4.3 Pesticides

In recent decades, the use of pesticides in agriculture has significantly increased due to the need to ensure higher crop yields and protect plants from pests, diseases, and weeds. While pesticides have contributed to food security, their excessive and indiscriminate application has led to serious environmental and health concerns. Many pesticides are persistent organic pollutants (POPs) that accumulate in soil, water bodies, and the food chain, resulting in toxicity to non-target organisms, including beneficial insects, birds, aquatic life, and even humans. Exposure to these chemicals has been linked to neurological disorders, endocrine disruption, and carcinogenic effects.[174,175] In response to these challenges, researchers have turned to nanotechnology-based solutions, particularly graphene oxide (GO)-based nanocomposites, for the remediation of pesticide-contaminated environments. Graphene oxide possesses a high surface area, excellent adsorptive capacity, and functional groups that can facilitate catalytic degradation reactions. When incorporated with metal or metal oxide nanoparticles, GO-based nanocomposites act as highly efficient photocatalysts under visible light, breaking down complex pesticide molecules into less harmful or inert compounds. This approach offers a promising, sustainable strategy for mitigating the environmental impact of pesticides while ensuring agricultural productivity.[176,177]

Dehghan *et al.*[178] synthesized an rGO@Fe_3O_4@ZnO nanocatalyst *via* the thermal co-precipitation method and further used it to study the oxidative degradation of the pesticide metalaxyl in aqueous solution under vis-light irradiation. It was found that under optimized conditions, a degradation of 92.11% was achieved in 120 min, along with good reusability and reduced toxicity of metalaxyl.

For the degradation of chlorpyrifos, an organophosphate pesticide, under visible light, Zangiabadi and co-workers[179] synthesized GO@Fe_3O_4@TiO_2 mesoporous nanocomposites as nanocatalysts. The nanocomposite showed great promise, achieving 97% degradation of the pesticide under investigation in 60 min. It also showed good catalytic activity after repeated runs, as it shows the possible degradation mechanism.

The degradation of chlorpyrifos under UV light was studied by Gupta *et al.*[51] who synthesized an rGO@$CoFe_2O_4$@TiO_2 photocatalyst using co-precipitation and modified Hummers' methods (Fig. 31–33). The nanocomposite showed good catalytic activity for the degradation of the given organophosphate pesticide along with good reusability.

The degradation of another pesticide, diazinon, was evaluated in a study by Naynava *et al.*[180] using a GO@Fe_3O_4@CeO_2 heterojunction based photocatalyst under visible light irradiation. The use of the nanocomposite showed great promise, degrading 97.9% of the organophosphate pesticide in 60 min (Fig. 34).

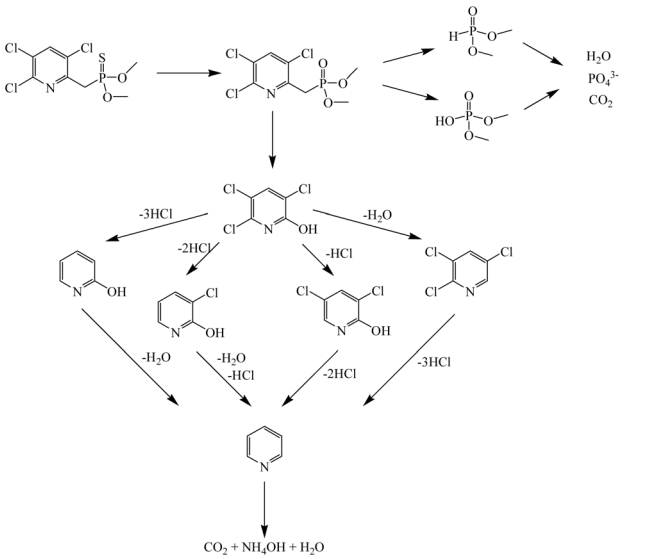

Fig. 31 A possible mechanism for the degradation of chlorpyrifos.

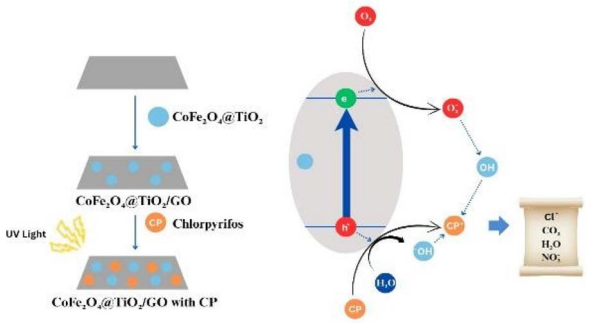

Fig. 32 Photocatalytic degradation mechanism of chlorpyrifos using the $rGO@TiO_2@CoFe_2O_4$ nanocomposite.

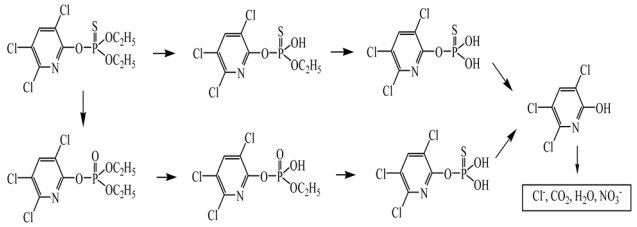

Fig. 33 Degradation pathways of chlorpyrifos using the $rGO@TiO_2@CoFe_2O_4$ nanocomposite.

The excessive use of herbicides in agriculture has been a growing problem due to the difficulties in removing them from the environment. Boruah and Das[181] studied the photometric detection and degradation of atrazine, a chlorinated herbicide belonging to the class of triazines, using an $rGO@Fe_3O_4@TiO_2$ nanocomposite prepared using the one-step hydrothermal method. The results indicated that the nanocomposite showed impressive capability to photocatalytically degrade the atrazine molecule, degrading 100% of the herbicide under natural sunlight irradiation (Fig. 35) The removal of the organochlorine insecticides aldrin and dieldrin from surface water using magnetically retrievable nanocomposites was investigated by Akçağlar,[182] who synthesized a $GO@CuFe_2O_4@TiO_2$ photocatalyst using hydrothermal and Hummers' methods(Fig. 36). It was found that under optimal conditions, photodegradation efficiencies of 100% and 99% were achieved for aldrin and dieldrin respectively, along with impressive reusability.

Nasiripur *et al.*[183] studied the photocatalytic degradation of the organophosphate insecticide parathion methyl using a $GO@Fe_3O_4@Bi_2MoO_6$ nanocomposite (Fig. 37 and 38).

$$GO/Fe_3O_4/CeO_2 + h\nu \longrightarrow h^+ + e^- \quad (1)$$

$$e^- + \text{Diazinon} \longrightarrow \text{Diazinon}^- \quad (2)$$

$$e^- + O_2 \longrightarrow O_2^- \quad (3)$$

$$O_2^- + e^- + 2H^+ \longrightarrow H_2O_2 \quad (4)$$

$$H_2O_2 + e^- \longrightarrow HO^+ + HO^- \quad (5)$$

$$HO^+ + \text{Diazinon} \longrightarrow \text{Diazinon}^+ \quad (6)$$

Fig. 34 Reactions showing the degradation pathway of diazinon.

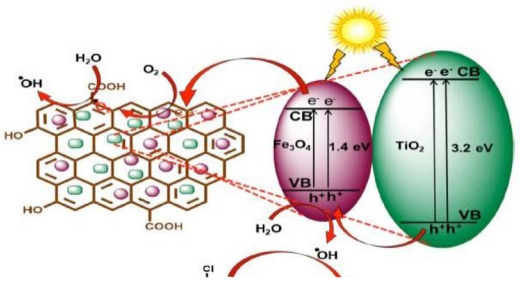

Fig. 35 Photocatalytic degradation of atrazine represented schematically. Reproduced from ref. 181 with permission from Elsevier, copyright 2020.

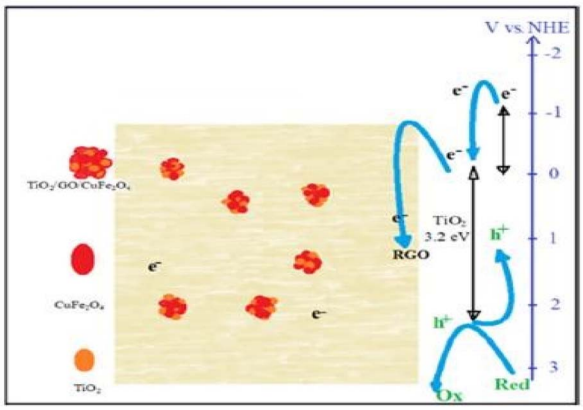

Fig. 36 Photocatalytic activity of a $GO@TiO_2@CuFe_2O_4$ nanocomposite.

Under suitable conditions, 95% of parathion methyl was degraded under visible light irradiation in 120 min. Binary nanocomposites containing magnetic oxides and ferrites in conjunction with GO have also been studied for the degradation of pesticides in aqueous media.

Tabasum and co-workers[184] designed $GO@MnFe_2O_4$ and $GO@NiFe_2O_4$ binary photocatalysts for the study of acetamiprid, an odourless neonicotinoid pesticide, and under UV methylene blue (MB) in wastewater was degraded using a $GO@MgFe_2O_4@CuO$ nanocomposite through a microwave-ultrasonic procedure. The synthesised photocatalysts showed excellent degradation capacity, degrading >90% of the pesticide in 27 min.

In similar research, Tabasum *et al.*[185] synthesized $GO@Fe_3O_4$ and $GO@CoFe_2O_4$ nanocomposites to study the degradation of the same pesticide. It was found that the ferrite and magnetite photocatalysts degraded approximately 97% and 90% of the acetamiprid pesticide respectively, in 60 min of UV light irradiation.

Khoj *et al.*[186] synthesized a $GO@Fe_3O_4$ binary nanocomposite and utilised it to investigate the degradation of the organophosphate pesticide diazinon. 99% of diazinon degradation was observed under 50 min of UV-light irradiation.

Persulphate-activated $GO@Fe_3O_4$ nanocomposites were prepared by Dolatabadi *et al.*[187] for the study of the degradation

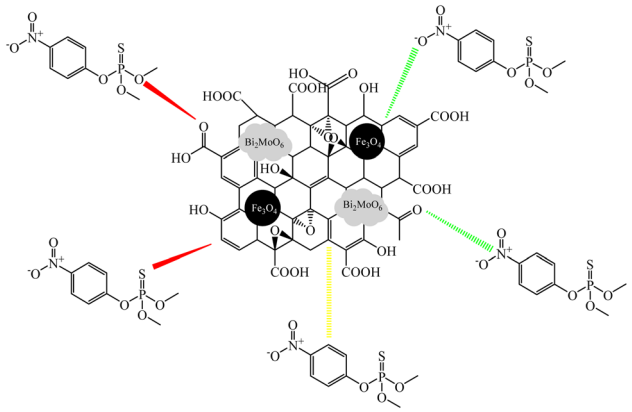

Fig. 37 Possible interaction between methyl parathion and a GO@Fe_3O_4@Bi_2MoO_6 nanocomposite.

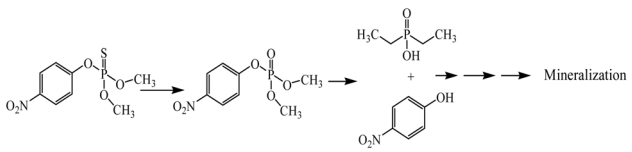

Fig. 38 Products obtained from photocatalytic degradation of methyl parathion.

of the organophosphate insecticide malathion in groundwater samples. The photocatalyst showed excellent capacity as a degrading agent, showing a degradation efficiency of 96.5% in 30 min of reaction.

Deviating slightly from standard research, Soltani-nezhad and coworkers[188] synthesized a quaternary nanocomposite GO@Fe_3O_4@TiO_2–NiO and studied the photocatalytic degradation of the pesticide imidacloprid under varying conditions of pH and nanocatalyst and pesticide concentrations. The results showed that under optimal conditions (pH: 9, 0.1 g nanocatalyst, and 25 ppm pesticide), 94.61% degradation was observed under visible light irradiation.

4.4 Dyes

The widespread rise in the use of artificial dyes, particularly in the textile, leather, paper, and cosmetic industries, has been driven by their bright colours, stability, and cost-effectiveness. However, this increased usage has led to significant environmental challenges. Many synthetic dyes are non-biodegradable and persist in the environment, especially in water bodies, where they reduce light penetration, hinder photosynthesis, and disrupt aquatic ecosystems. Additionally, several dyes and their degradation products are toxic, mutagenic, or even carcinogenic, posing serious health risks to humans and animals. Conventional methods for dye removal, such as coagulation, flocculation, or adsorption using activated carbon, often have limitations in efficiency and cost.[189,190] In recent years, graphene oxide (GO)-based nanocomposites have emerged as promising materials for the degradation of artificial dyes. Due to GO's high surface area, abundant functional groups, and excellent dispersibility in aqueous media, it serves as an effective support for metal and metal oxide nanoparticles. These nanocomposites can act as powerful photocatalysts under sunlight or visible light, accelerating the breakdown of complex dye molecules into less harmful compounds. This green and efficient approach offers a sustainable solution to mitigate the environmental impact of artificial dye pollution.[191,192]

Waheed *et al.*[193] studied the photocatalytic degradation of methylene blue (MB) in wastewater using a GO@$MgFe_2O_4$@-CuO nanocomposite synthesized through a microwave-ultrasonic procedure. The synthesized nanocatalyst, under optimal conditions, showed a degradation efficiency of 98.8% in 27 min and also showed good reusability up to four cycles of the photocatalytic degradation process.

Benjwal *et al.*[194] investigated the photocatalytic degradation of MB using binary rGO@TiO_2 and rGO@Fe_3O_4 and tertiary rGO@Fe_3O_4@TiO_2 nanocomposites synthesized from a one-step solvothermal process, and the catalytic activity of each nanocomposite was compared. Under visible and UV light irradiation, 100% and 91% MB degradation were observed respectively, within 5 min for the ternary nanocomposite, showcasing its superior capability as a photocatalyst in comparison to binary nanocomposites.

Banerjee and co-workers[195] also conducted the experiment using the same dye and ternary nanocomposite. Different component ratios of the rGO@Fe_3O_4@TiO_2 photocatalyst were synthesized using sol–gel and wet assembly methods. It was found that the composite possessing the ratio 1 : 1 : 2 of rGO, Fe_3O_4 and TiO_2 showed the highest degradation of MB, degrading 99% and 94% of the sample under UV and visible light irradiation respectively (Table 2, Fig. 39).

In similar research, Nadimi *et al.*[196] independently conducted the same experiment, replacing rGO with GO. The nanocomposites were synthesized using modified Hummers' and

Table 2 Photocatalytic degradation efficiencies of different rGO@Fe_3O_4@TiO_2 nanocomposites

Nanocomposites	Photocatalytic degradation of MB under UV/visible light C/C_0 (%) (in 9 min)	C/C_0(%) (in 6 min)
GFT1	87	90
GFT2	93	95
GFT3	90	88
GFT4	90	97
GFT5	88	92
GFT6	94	99
GFT7	93	97

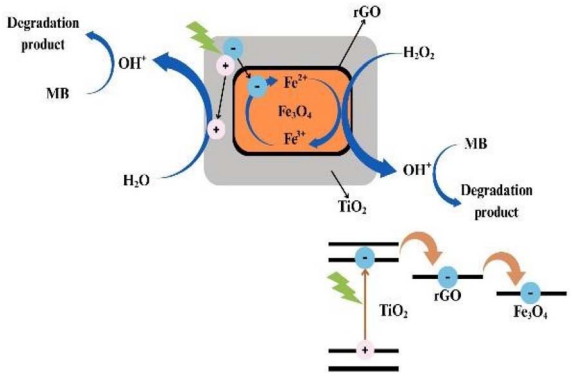

Fig. 39 Suggested mechanism for methylene blue degradation by the rGO@Fe_3O_4@TiO_2 nanocomposite.

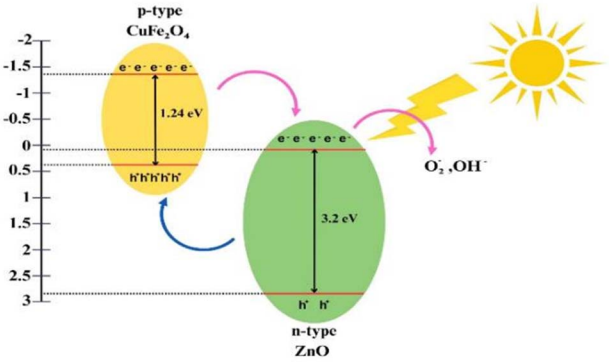

Fig. 40 Diagrammatic representation of photocatalytic degradation of a GO@ZnO@$CuFe_2O_4$ nanocomposite.

ultrasonication methods while varying the amount of GO. It was found that the nanocomposite with the highest amount of GO showed the greatest degradation of MB, with reported degradation percentages of 82% and 76% in 90 min of irradiation with UV and visible light respectively.

Bibi *et al.*[197] used the same rGO@Fe_3O_4@TiO_2 nanocomposite to study the photocatalytic degradation of the triarylmethane dye malachite green (MG) under UV-visible light. The conventional hydrothermal method was used to synthesize the photocatalyst. The results showed that, in comparison to pure TiO_2, the nanocomposite showed much greater promise as a photocatalyst, degrading 99% of MG in 55 min under visible light irradiation.

Ojha and co-workers[198] investigated the photocatalytic degradation of an azo-dye from an aqueous medium under ambient conditions utilizing an rGO@Fe_3O_4@ZnO nanocomposite synthesized using the hydrothermal method. The catalytic activities of the tertiary nanocomposites were compared to those of pure ZnO, pure Fe_3O_4, ZnO@Fe_3O_4 and Fe_3O_4@GO systems. It was found that the nanocomposites showed superior degradation capability, attributed to the synergistic effect of the components of the nanoparticles, degrading approximately 97% of the azo-dye within 150 min of visible light irradiation.

Kumar *et al.*[199] synthesized GO@$CuFe_2O_4$@ZnO nanocomposites using a one-step combustion process (Fig. 40) for the study of photocatalytic degradation of MB, the azo-dye methyl orange (MO) and the xanthene dye rhodamine-B (RhB). The separation ratio of the photogenerated electron–hole pairs was enhanced due to the generation of a p–n junction between $CuFe_2O_4$ and ZnO. The ternary nanocomposite showed great promise, degrading 99% of RhB in 50 min, 100% of MB in 40 min and >90% of MO in 200 min.

The photocatalytic degradation of Bismarck Brown (BB) and Acid Orange 7 (AO7) was studied by Boruah *et al.*[79] using an rGO@Fe_3O_4@V_2O_5 nanocomposite synthesized through the co-precipitation method. It was found that 94.5% of BB and 93.3% of AO were degraded using the photocatalyst in 70 and 80 min respectively.

Similar to the work on pesticides, binary nanocomposites composed of magnetic oxides or ferrites embedded in graphene oxide have also been studied for their role in the photocatalytic degradation of dyes in aqueous media. Baptisttella *et al.*[200] studied the degradation of various dyes such as MB, Reactive Black 5 (RB5) and Acid Blue 80 (AB80) using a GO@Fe_3O_4 binary nanocomposite. Degradation rates of 70%, 54% and 48% were obtained for MB, RB, and AB respectively.

GO-supported ferrites of Fe, Co and Ni (GO@$FeFe_2O_4$, GO@$CoFe_2O_4$, and GO@$NiFe_2O_4$) were synthesized by Sheshmani *et al.*[201] for the photocatalytic degradation of Remazol Black B (RBB). All three nanocomposites showed great promise as photocatalysts for the decomposition of the dye under study (Fig. 41).

5. Mechanism of photocatalytic degradation

A detailed analysis of the mechanism involved in the photocatalytic degradation of various organic pollutants reveals/indicates that upon light irradiation, the metal oxide semiconductor component of the photocatalyst generates e^-/h^+ pairs. These photo-generated electrons in the conduction band reduce oxygen to superoxide radicals ($^{\bullet}O_2^-$) and water to

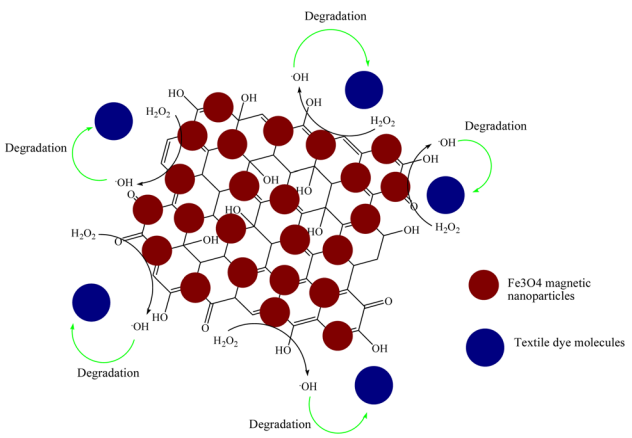

Fig. 41 Schematic representation of the possible photocatalytic degradation mechanism of dyes.

Table 3 A critical comparison of photocatalytic activity of unmodified metal oxide photocatalysts and MMO@GO nanocomposites

S no.	Pollutant class		Photocatalyst	Target pollutant	Photocatalyst separation	Light source	Degradation efficiency (%)	Time (in min)	No of recovery cycles	Ref.
1	Pharmaceutical	Antimicrobial	TiO_2-P25	Tetracycline	Centrifugation	UV/visible	25.1	120	4	209
			ZnO	Ciprofloxacin	Filtration	UV	50	60	—	210
			ZnO	Oxytetracycline	Filtration	UV	76.1	80	—	211
			$CuFe_2O_4$/rGO	Tetracycline	Magnetic separation	Visible	90.44	160	5	111
			Co_3O_4/TiO_2/GO	Oxytetracycline	Magnetic separation	UV/visible	91	90	5	119
			GO@Fe_3O_4@TiO_2	Ciprofloxacin	Magnetic separation	UV/visible	91.5	240	5	123
			TiO_2/Fe_2O_3/GO	Metronidazole	Magnetic separation	UV/visible	97	120	—	124
		Psychopharmaceutical	H_2TiO_7 nanotubes	Clonazepam	Centrifugation	—	80.79	240	4	212
			rGO/TiO_2/CSA	Caffeine and carbamazepine	Magnetic separation	UV/visible	99	60	10	141
			Fe_3O_4-graphene oxide	Clonazepam	Magnetic separation	UV	100	5	5	142
		Antipyretic	TiO_2 P25	Paracetamol	Centrifugation	UV	90	150	4	213
			rGO/BSO/g-C_3N_4	Naproxen	Filtration	UV	77.52	90	4	214
			Fe_3O_4@Mn_3O_4-rGO	Sulfamethazine	Magnetic separation	UV	98	120	—	127
		Estrogen	TiO_2	Estrone-3-glucuronide	Filtration	UV	25	390	—	215
			$ZnFe_2O_4$-Ag/rGO	17α-Ethinylestradiol	Magnetic separation	UV	80	240	5	148
		Antidiabetic	TiO_2-ZrO_2	Metformin	Centrifugation	UV	50	30	—	216
			Fe_3O_4@rGO@ZnO/Ag	Metformin	Magnetic separation	Visible	100	60	5	152
2	Microplastics		GO@metal oxide	Polyethylene	Centrifugation	UV	10.3	480	—	217
			Fe_3O_4@TiO_2/Ag	Polyethylene	Centrifugation	UV	17.54	180	5	218
3	Pesticide		GO-TiO_2	Atrazine	Filtration	UV/visible	50	59	—	219
			rGO@Fe_3O_4@ZnO	Metalaxyl	Magnetic separation	Visible	92	120	5	179
			GO@Fe_3O_4@TiO_2	Chlorpyrifos	Magnetic separation	Visible	97	60	4	180
			GO@Fe_3O_4@CeO_2	Diazinon	Magnetic separation	Visible	97.9	60	5	182
4	Dye		Co_3O_4/ZnO	Methylene blue	Centrifugation	—	86	90	—	220
			ZnO/$NiFe_2O_4$	Methylene blue	—	—	93	70	—	221
			rGO@Fe_3O_4@TiO_2	Methylene blue	Magnetic separation	Visible	100	5	5	195
			rGO@Fe_3O_4@V_2O_5	Acid orange 7	Magnetic separation	Visible	93.3	70	5	79
			rGO@Fe_3O_4@V_2O_5	Bismarck brown	Magnetic separation	Visible	94.3	70	5	79

hydroxyl radicals ($^{\bullet}OH$).[202] Though the efficiency is reduced due to rapid recombination of these e^-/h^+ pairs, to mitigate this challenge, graphene oxide or reduced graphene oxide (GO or rGO) plays a pivotal role. The incorporation of graphene oxide or reduced graphene oxide (GO or rGO) introduces an interfacial electron transfer pathway to facilitate the migration of photo-generated electrons from the metal oxide conduction band to GO. This electron trapping suppresses charge recombination leading to enhanced radical formation and consequently improved degradation efficiency.[203,204]

To understand the mechanism of action of these radical intermediates, many chemical species able to interact with them have been applied to various oxidative processes. Such substances are termed "radical scavengers", capable of reacting quickly and specifically with a radical to form a stable species which does not interfere in the reaction. Various molecules have been studied for the radical scavenging of different intermediates: for example, holes in the valence band are scavenged using electron donating species such as ethylene glycol,[205] hydroxyl radicals ($^{\bullet}OH$) can be scavenged by flavonoids,[206] and superoxide ion radicals ($^{\bullet}O_2^-$) can be scavenged by ascorbic acid.[207] Scavengers would be useful in identifying the dominant active species responsible for the degradation of pollutants and hence help in understanding the mechanistic pathway for the degradation.

Disi Qiao *et al.*[115] did mechanistic studies for photocatalytic degradation of tetracycline using an Fe_3O_4@GO@ZnO nanocomposite using 5,5-dimethyl-1-pyrroline-*N*-oxide (DMPO) as a scavenger. They reported the presence of DMPO-$^{\bullet}OH$ and DMPO-$^{\bullet}O_2^-$ in the Electron Spin Resonance (ESR) spectra indicating the dual effects of $^{\bullet}OH$ radicals and $^{\bullet}O_2^-$ radicals during the photocatalytic degradation. Similar studies employing DMPA and TEMPO as scavengers were done on a C_3N_4@MnO_2@GO nanocomposite by Chunyan Du *et al.*[116] demonstrating that the presence of h^+ also played a role in the system apart from $^{\bullet}OH$ radicals and $^{\bullet}O_2^-$ radicals. Furthermore, in the presence of peroxide, if the composite contains an iron species, enhanced generation of $^{\bullet}OH$ is observed.[117]

Summarizing the discussions, scavenger studies reveal that hydroxyl ($^{\bullet}OH$) radicals and superoxide ($^{\bullet}O_2^-$) radicals are the primary reactive oxygen species while the contribution of valence band holes[208] is dependent on the relative positions of the edge gap of the valence band. Notably in many reported systems superoxide radicals behave as the primary ROS due to efficient electron migration to GO. Therefore, the enhanced photocatalytic efficiency of magnetic MO@GO nanocomposites can be attributed to effective electron trapping, reduced electron–hole recombination and enhanced radical generation with the superoxide radical being the primary ROS.

6. Comparison with other catalysts

To date, many heterogeneous photocatalytic systems have been developed for the degradation of organic pollutants. However, magnetically retrievable metal oxide@graphene oxide systems have garnered immense attraction due to their brilliant efficiency, ease of separation, *etc.* Table 3 lists comparative data of the parameters associated with the degradation process for different metal oxide based photocatalysts and magnetic metal oxide@graphene oxide-based systems. Even though these nanocomposite systems can be a bit expensive, when compared to unmodified metal oxides they show higher degradation efficiency and similar recovery cycles showcasing stability under aqueous conditions, and in several cases, they can degrade organic pollutants under visible light irradiation, increasing their utility in real world. These characteristics coupled with the ease of separation make them a viable candidate for water remediation *via* degradation of organic pollutants. Despite these advantages, concerns have been raised against the toxicity of the different components of these nanocomposites; therefore the effects of the long-term exposure of these nanocomposites on human health and the environment need to be further studied.

7. Challenges, future research, directions and SWOT analysis of metal oxide @graphene oxide nanocomposites

Magnetic MMO nanocomposites represent a promising class of engineered materials with wide ranging applications in catalysis, energy storage, environmental remediation and sensing technologies. However, despite their immense potential, the transition from laboratory-scale to large scale operations presents a new set of scientific, technological, and environmental challenges. In this regard, a systematic SWOT (Strengths, Weaknesses, Opportunities, Threats) analysis becomes essential to highlight the current state and future trajectory of these nanocomposites.

The primary strengths of these nanocomposites lie in their multifunctional characteristics, which include improved magnetic properties, tunable electronic properties, large surface area, high efficiency, thermal and chemical stability, reusability and mechanical robustness.[25,26,222–224] Despite these advantages, significant weaknesses require considerable attention. The most critical challenge is the lack of scalable, reproducible, and environmentally benign synthesis methods. Many current strategies involve complex, multi-step processes involving toxic reagents or harsh conditions, which are incompatible with large-scale manufacturing.[225] Homogeneous dispersion of metal oxide nanoparticles on GO sheets is difficult to achieve due to aggregation of MO. This directly impacts the performance consistency of the resulting photocatalyst.[226] Another fundamental weakness is charge recombination which although mitigated by GO, still appears, especially in composites with suboptimal interfacial contact or excessive GO loading that can shield active sites.[222] Additionally, studies regarding the long-term structural stability and catalyst recyclability under various conditions (*e.g.* in aqueous environments of varying matrix composition or pH or at different temperatures) are often limited. Nanoparticles can leach out and the GO support may degrade over multiple cycles under diverse conditions leading to performance decay.[227]

These weaknesses point directly to key opportunities for future research. There is a need for the development of green, one pot synthesis strategies that are energy-efficient, use water as a solvent and avoid hazardous chemicals. These include methods such as hydrothermal, solvothermal, or mechanochemical based synthesis.[228,229] Research should focus on engineering the MMO–GO interface at the atomic level to maximize charge transfer efficiency and minimize recombination losses. This may include covalent functionalization or the creation of heterojunctions with tailored band alignments. Another major opportunity lies in designing hierarchical or 3D architectures (*e.g.*, aerogels and foams) that can prevent restacking of GO sheets while retaining high surface area, facilitating mass transport.[230] Furthermore, integrating MMO@GO composites into practical devices, such as flow reactors for water treatment, represents an important step toward real-world application.[231]

However, these opportunities are associated with serious threats that need to be addressed.

The foremost threat is the potential environmental and health impact of these nanomaterials. The long-term ecotoxicity of these nanocomposites, their persistence in ecosystems, and their potential to bioaccumulate are not yet fully understood.[232] Without comprehensive life-cycle assessments and clear regulatory frameworks, public and governmental acceptance represents a significant barrier. Another threat is the economic viability of large-scale production. High cost of superior quality GO and complexity of controlled synthesis may render these materials too expensive for many applications compared to conventional materials.

While MMO@GO nanocomposites possess a remarkable set of strengths that makes them ideal candidates for next-generation technologies, their real-world applications depend upon overcoming substantial weaknesses in synthesis and stability. Through innovation in green manufacturing and advanced architecture design while actively addressing the threats related to environmental safety and economic feasibility, the full potential of these materials can be harnessed. Future research must adopt a holistic, interdisciplinary approach encompassing materials chemistry, process engineering, and environmental science to ensure their sustainable and responsible development.

8. Conclusions

The evolution of nanocomposites based on the integration of magnetic compounds, such as oxides and ferrites into graphene oxide nanosheets along with metal oxides, is a transformative approach towards the sustainable photocatalytic degradation of organic pollutants in aqueous media. By leveraging the high surface area, electron mobility, and functional versatility of graphene oxide with the redox activity and UV and visible-light responsiveness of engineered metal oxides, such systems offer enhanced charge separation, prolonged catalyst lifetime, and superior degradation efficiencies. In this review, we have discussed various methods for the synthesis of magnetically retrievable metal oxide/graphene oxide and metal oxide/reduced graphene oxide nanocomposites, their application as photocatalysts in the degradation of pharmaceuticals, microplastics, pesticides and dyes in aqueous media, and their role in various organic transformations. The synergistic integration of metal oxides, graphene oxide, and ferrite nanoparticles in nanocomposite systems plays a crucial role in enhancing catalytic activity and improving pollutant removal efficiency. The literature reviewed in this study demonstrates that these composite materials exhibit remarkable degradation performance, often achieving up to 100% pollutant removal within a short reaction time under optimized conditions. Moreover, their excellent stability and reusability, with minimal loss of catalytic activity over multiple cycles, make them highly promising candidates for sustainable water treatment technologies. Therefore, such integrated nanocomposite systems represent a significant advancement in the field of environmental remediation and offer strong potential for future development in efficient and cost-effective wastewater treatment applications.

Author contributions

AS, SD, RKS and RJ were involved in the conceptualization and design of the work. SD, PK, Kirti, RS and Priyanka contributed to reviewing and editing the manuscript. Kirti, VKU, Geetanshu and SNK were involved in the literature review, data curation and writing of the manuscript.

Conflicts of interest

There are no conflicts to declare.

Data availability

No new data were generated; hence, data sharing is not applicable to this article.

Acknowledgements

Kirti would like to thank CSIR for the award of a Senior Research Fellowship. All the authors would like to thank Hindu College for the award of the Lalit Kumar Jain Memorial Research Fellowship.

References

1 N. Morin-Crini, E. Lichtfouse, G. Liu, V. Balaram, A. R. L. Ribeiro, Z. Lu, F. Stock, E. Carmona, M. R. Teixeira, L. A. Picos-Corrales, J. C. Moreno-Piraján, L. Giraldo, C. Li, A. Pandey, D. Hocquet, G. Torri and G. Crini, *Environ. Chem. Lett.*, 2022, **20**, 2311–2338.
2 L. Lin, H. Yang and X. Xu, *Front. Environ. Sci.*, 2022, **10**, 880246.
3 R. Fuller, P. J. Landrigan, K. Balakrishnan, G. Bathan, S. Bose-O'Reilly, M. Brauer, J. Caravanos, T. Chiles, A. Cohen, L. Corra, M. Cropper, G. Ferraro, J. Hanna, D. Hanrahan, H. Hu, D. Hunter, G. Janata, R. Kupka, B. Lanphear, M. Lichtveld, K. Martin, A. Mustapha,

E. Sanchez-Triana, K. Sandilya, L. Schaefli, J. Shaw, J. Seddon, W. Suk, M. M. Téllez-Rojo and C. Yan, *Lancet Planet. Health*, 2022, **6**, e535–e547.
4 A. Mandal, P. Senthil Kumar, C. S. Poorva, L. Srinivasa Raju, S. R. Balasubramani and G. Rangasamy, *Water Pract. Technol.*, 2024, **19**, 937–959.
5 K. C. Jones and P. de Voogt, *Environ. Pollut.*, 1999, **100**, 209–221.
6 M. A. Ashraf, *Environ. Sci. Pollut. Res.*, 2017, **24**, 4223–4227.
7 A. B. T. Akhtar, S. Naseem, A. Yasar and Z. Naseem, in *Environmental Pollution and Remediation*, Springer, 2021, pp. 213–246.
8 W. A. H. Altowayti, S. Shahir, N. Othman, T. A. E. Eisa, W. M. S. Yafooz, A. Al-Dhaqm, C. Y. Soon, I. B. Yahya, N. A. N. b. Che Rahim, M. Abaker and A. Ali, *Processes*, 2022, **10**, 1832.
9 A. T. Nguyen and L. Le Tran, *Rev. Environ. Contam. Toxicol.*, 2024, **262**, 11.
10 A. Al Miad, S. P. Saikat, M. K. Alam, M. S. Hossain, N. M. Bahadur and S. Ahmed, *Nanoscale Adv.*, 2024, **6**, 4781–4803.
11 X. Zhang, Y. L. Chen, R. S. Liu and D. P. Tsai, *Rep. Prog. Phys.*, 2013, **76**, 046401.
12 R. Schlögl and S. B. Abd Hamid, *Angew. Chem., Int. Ed.*, 2004, **43**, 1628–1637.
13 P. Christopher, D. B. Ingram and S. Linic, *J. Phys. Chem. C*, 2010, **114**, 9173–9177.
14 L. L. Zhang, Z. Xiong and X. S. Zhao, *ACS Nano*, 2010, **4**, 7030–7036.
15 G. Williams, B. Seger and P. V. Kamat, *ACS Nano*, 2008, **2**, 1487–1491.
16 K. C. Kemp, H. Seema, M. Saleh, N. H. Le, K. Mahesh, V. Chandra and K. S. Kim, *Nanoscale*, 2013, **5**, 3149–3171.
17 F. T. Geldasa, M. A. Kebede, M. W. Shura and F. G. Hone, *RSC Adv.*, 2023, **13**, 18404–18442.
18 T. Velempini, E. Prabakaran and K. Pillay, *Mater. Today Chem.*, 2021, **19**, 100380.
19 K. H. Kumar, H. T. Ananda, D. K. Ravishankar, H. Madhu and S. Thirumala, *Sustain. Chem. One World*, 2025, 100055.
20 X. Hong, X. Wang, Y. Li, J. Fu and B. Liang, *Catalysts*, 2020, **10**, 921.
21 K. Q. Lu, Y. H. Li, Z. R. Tang and Y. J. Xu, *ACS Mater. Au*, 2021, **1**, 37–54.
22 C. Rios, L. Bazán-Díaz, C. A. Celaya, R. Salcedo and P. Thangarasu, *Molecules*, 2023, **28**, 7331.
23 Y. Feng, X. Su, Y. Chen, Y. Liu, X. Zhao, C. Lu, Y. Ma, G. Lu and M. Ma, *Mater. Res. Bull.*, 2023, **162**, 112207.
24 A. Singh, D. Singh, B. Ahmed and A. K. Ojha, *Mater. Chem. Phys.*, 2022, **277**, 125531.
25 P. Majumder and R. Gangopadhyay, *RSC Adv.*, 2022, **12**, 5686–5719.
26 N. Mushahary, A. Sarkar, F. Basumatary, S. Brahma, B. Das and S. Basumatary, *Results Surf. Interfaces*, 2024, **15**, 100225.
27 P. Das, C. R. Penton, P. Westerhoff and F. Perreault, *Environ. Sci.: Nano*, 2023, **10**(11), 2936–2956.
28 S. K. Sharma and S. Sharma, *Chem. Eng. Technol.*, 2025, **48**, e70009.
29 B. Anegbe, I. H. Ifijen, M. Maliki, I. E. Uwidia and A. I. Aigbodion, *Environ. Sci. Eur.*, 2024, **36**, 15.
30 Y. Wei, G. Duan, Y. Huang, X. Han, C. Zhang, S. He, H. Zhao, C. Ma and S. Jiang, *J. Water Proc. Eng.*, 2025, **74**, 107766.
31 M. U. Farooq and M. I. Jalees, *J. Water Proc. Eng.*, 2020, **33**, 101044.
32 B. Bhushan, P. Negi, A. Nayak and S. Goyal, *Adv. Compos. Hybrid Mater.*, 2024, **8**, 55.
33 S. Abbasi, *Appl. Water Sci.*, 2023, **13**, 128.
34 S. Rajendrakumar, D. Mavhaire, S. Shimly, N. Tharanidevi, V. S. Ramachandran and R. R. Timilsina, Drivers and barriers towards achieving SDG 6 on clean water and sanitation for all-an Indian perspective, *World Development Sustainability*, 2025, **7**, 100228.
35 S. Singh and R. Jayaram, Attainment of water and sanitation goals: a review and agenda for research, *Sustain. Water Resour. Manag.*, 2022, **8**(5), 146.
36 M. Nikazar, M. Alizadeh, R. Lalavi and M. H. Rostami, *J. Environ. Health Sci. Eng.*, 2014, **12**, 21.
37 W. S. Hummers, Jr. and R. E. Offeman, *J. Am. Chem. Soc.*, 1958, **80**, 1339.
38 D. C. Marcano, D. V. Kosynkin, J. M. Berlin, A. Sinitskii, Z. Sun, A. Slesarev, L. B. Alemany, W. Lu and J. M. Tour, *ACS Nano*, 2010, **4**, 4806–4814.
39 S. Abbasi, F. Ahmadpoor, M. Imani and M.-S. EkramiKakhki, *Int. J. Environ. Anal. Chem.*, 2020, **100**, 225–240.
40 R. Eivazzadeh-Keihan, R. Taheri-Ledari, N. Khosropour, S. Dalvand, A. Maleki, S. M. Mousavi-Khoshdel and H. Sohrabi, *Colloids Surf., A*, 2020, **587**, 124335.
41 A. Bateni, K. Valizadeh, Y. Salahshour, A. H. Behroozi and A. Maleki, *J. Environ. Manage.*, 2022, **324**, 116358.
42 N. Salimi, E. Mohammadi-Manesh, N. Ahmadvand, H. Danafar and S. Ghiasvand, *J. Inorg. Organomet. Polym. Mater.*, 2024, **34**, 1256–1271.
43 C. B. Anucha, I. Altin, E. Bacaksiz and V. N. Stathopoulos, *Chem. Eng. J. Adv.*, 2022, **10**, 100262.
44 K. Nakata and A. Fujishima, *J. Photochem. Photobiol. C Photochem. Rev.*, 2012, **13**, 169–189.
45 M. Cao, P. Wang, Y. Ao, C. Wang, J. Hou and J. Qian, *Chem. Eng. J.*, 2015, **264**, 113–124.
46 Z.-J. Li, Z.-W. Huang, W.-L. Guo, L. Wang, L.-R. Zheng, Z.-F. Chai and W.-Q. Shi, *Environ. Sci. Technol.*, 2017, **51**, 5666–5674.
47 B. K. Ghosh, D. Moitra, M. Chandel and N. N. Ghosh, *J. Nanosci. Nanotechnol.*, 2017, **17**, 4694–4703.
48 Q. Li, H. Kong, P. Li, J. Shao and Y. He, *J. Hazard Mater.*, 2019, **373**, 437–446.
49 J. Mehralipour, S. Bagheri and M. Gholami, *Heliyon*, 2023, **9**(7), e18172.
50 D. Bala, I. Matei, G. Ionita, D.-V. Cosma, M.-C. Rosu, M. Stanca, C. Gaidau, M. Baleanu, M. Virgolici and I. Stanculescu, *Int. J. Mol. Sci.*, 2022, **23**, 14703.
51 V. K. Gupta, T. Eren, N. Atar, M. L. Yola, C. Parlak and K. M. Hassan, *J. Mol. Liq.*, 2015, **208**, 122–129.

52 X. Zhang, P. Yu, Y. Chen and Y. Ma, *Mater. Lett.*, 2010, **64**, 583–585.
53 D. Liu, B. B. Garcia, Q. Zhang, Q. Guo, Y. Zhang, S. Sepehri and G. Cao, *Adv. Funct. Mater.*, 2009, **19**, 1015–1023.
54 M. Zhou, X. Zhang, J. Wei, S. Zhao, L. Wang and B. Feng, *J. Phys. Chem. C*, 2011, **115**, 1398–1402.
55 L. Zhang, J. Lian, L. Wu, Z. Duan, J. Jiang and L. Zhao, *Langmuir*, 2014, **30**, 7006–7013.
56 X. Chen, Y.-F. Shen, S. L. Suib, C. B. Zhi, H. Ding, D. Wang, Y. Cao, Y. Zhang, X. Wang, Y. Liu and Q. Huo, *J. Mater. Chem. A*, 2014, **2**, 2374–2382.
57 B. Zhi, H. Ding, D. Wang, Y. Cao, Y. Zhang, X. Wang, Y. Liu and Q. Huo, *J. Mater. Chem. A*, 2014, **2**, 2374–2382.
58 Q. Tang, M. Sun, S. Yu and G. Wang, *Electrochim. Acta*, 2014, **125**, 488–496.
59 J. Tang, M. Myers, K. A. Bosnick and L. E. Brus, *J. Phys. Chem. B*, 2003, **107**, 7501–7506.
60 Y. Liu, C. Luo, G. Cui and S. Yan, *RSC Adv.*, 2015, **5**, 54156–54164.
61 L. Tan, J. Wang, Q. Liu, Y. Sun, X. Jing, L. Liu, J. Liu and D. Song, *New J. Chem.*, 2015, **39**, 868–876.
62 J. Li, Y. Chen, Q. Wu and H. Xu, *J. Alloys Compd.*, 2017, **693**, 373–380.
63 B. M. Weckhuysen and D. E. Keller, *Catal. Today*, 2003, **78**, 25–46.
64 M. Shanmugam, A. Alsalme, A. Alghamdi and R. Jayavel, *ACS Appl. Mater. Interfaces*, 2015, **7**, 14905–14911.
65 P. K. Boruah, S. Szunerits, R. Boukherroub and M. R. Das, *Chemosphere*, 2018, **191**, 503–513.
66 F. Jafari and F. R. Rahsepar, *ACS Omega*, 2023, **8**, 35427–35439.
67 W. M. Husain, J. K. Araak and O. M. Ibrahim, *Iraqi J. Vet. Med.*, 2019, **43**, 6–14.
68 R. A. Salman, *Ibn al-Haitham J. Pure Appl. Sci.*, 2018, **31**, 9–14.
69 A. J. Katafa and M. K. Hamid, *Iraqi J. Sci.*, 2020, 540–549.
70 N. J. Hattab, E. E. Laibi and M. M. Mohammed, *Ibn al-Haitham J. Pure Appl. Sci.*, 2024, **37**, 316–332.
71 A. F. Abdlzhra, I. A. Abdllatief and E. E. L. Alabodi, *Ibn al-Haitham J. Pure Appl. Sci.*, 2016, **29**, 379–389.
72 N. Horti, M. Kamatagi, S. Nataraj, M. Sannaikar and S. Inamdar, *AIP Conf. Proc.*, 2020, 2274.
73 R. Chintaparty, B. Palagiri, R. R. Nagireddy and V. S. R. I. Reddy, *Phase Transitions*, 2015, **88**, 929–938.
74 J. Park, J. C. Hwang, G. G. Kim and J. U. Park, *InfoMat*, 2020, **2**, 33–56.
75 J. K. Patel, A. Patel and D. Bhatia, in *Emerging Technologies for Nanoparticle Manufacturing*, Springer, 2021, pp. 3–23.
76 N. M. El-Shafai, M. E. El-Khouly, M. El-Kemary, M. S. Ramadan and M. S. Masoud, *RSC Adv.*, 2018, **8**, 13323–13332.
77 A. F. Ismail and E. E. Al Abodi, *Adv. J. Chem.*, 2025, **8**(3), 615–627.
78 S. Todorova, J.-L. Cao, D. Paneva, K. Tenchev, I. Mitov, G. Kadinov, Z.-Y. Yuan and V. Idakiev, in *Studies in Surface Science and Catalysis*, Elsevier, 2010, vol. 175, pp. 547–550.
79 N. Ghassemi, S. S. H. Davarani and H. R. Moazami, *J. Mater. Sci.: Mater. Electron.*, 2018, **29**, 12573–12583.
80 V. A. Tran, T. L. H. Nguyen and V.-D. Doan, *Chemosphere*, 2021, **270**, 129417.
81 K. H. P. Ngoc and A.-T. Vu, *Adsorpt. Sci. Technol.*, 2022, **2022**, 6454354.
82 P. Xu, P. Wang, X. Li, R. Wei, X. Wang, C. Yang, T. Shen, T. Zheng and G. Zhang, *Chem. Eng. J.*, 2022, **440**, 135863.
83 Y. Jain, M. Kumari, R. P. Singh, D. Kumar and R. Gupta, *Catal. Lett.*, 2020, **150**, 1142–1154.
84 N. Nasseh, F. S. Arghavan, N. Daglioglu and A. Asadi, *Environ. Sci. Pollut. Res.*, 2021, **28**, 19222–19233.
85 A. Di Bartolomeo, L. Iemmo, F. Giubileo, G. Luongo, F. Urban and A. Grillo, *Funct. Mater*, 2018, **28**, 1800657.
86 W. Fu, X. Xu, W. Wang, J. Shen and M. Ye, *ACS Sustain. Chem. Eng.*, 2018, **6**, 8935–8944.
87 M. Park, Y. J. Park, X. Chen, Y. K. Park, M. S. Kim and J. H. Ahn, *Adv. Mater.*, 2016, **28**, 2556–2562.
88 J. Yan, Z. Chen, H. Ji, Z. Liu, X. Wang, Y. Xu, X. She, L. Huang, L. Xu and H. Xu, *Chem. – Eur. J.*, 2016, **22**, 4764–4773.
89 S. Zhang, R. Hu, P. Dai, X. Yu, Z. Ding, M. Wu, G. Li, Y. Ma and C. Tu, *Appl. Surf. Sci.*, 2017, **396**, 994–999.
90 W. Yin, L. Yan, J. Yu, G. Tian, L. Zhou, X. Zheng, X. Zhang, Y. Yong, J. Li and Z. Gu, *ACS Nano*, 2014, **8**, 6922–6933.
91 W. Zhou, Y. Zhang, Y. Li, Y. Gou and X. Zhou, *Ceram. Int.*, 2022, **48**, 1908–1915.
92 X. Han, Y. Huang, J. Wang, X. Du, L. Hu, T. Li and X. Sun, *Composites, Part B*, 2022, **239**, 109965.
93 N. Liu, Y. Dou, X. Zhang, L. Yu and X. Yan, *Carbon*, 2022, **190**, 125–135.
94 D. Mu, Z. Chen, H. Shi and N. Tan, *RSC Adv.*, 2018, **8**, 36625–36631.
95 S. Tajik, A. A. Afshar, S. Shamsaddini, M. B. Askari, Z. Dourandish, F. Garkani Nejad, H. Beitollahi and A. Di Bartolomeo, *Ind. Eng. Chem. Res.*, 2022, **62**, 4473–4480.
96 X. Ding, G. Fan, Y. Huang and J. Wang, *J. Mater. Sci.: Mater. Electron.*, 2021, **32**, 9640–9649.
97 Z. Wang, 3-D flower-like (MoS2/Fe3O4)@rGO composite with multi-level structures for enhanced microwave absorption performance, in *SSRN*, 2022, DOI: 10.2139/ssrn.4217615.
98 S. Cherukulappurath and S. R. Amonkar, *Mater. Chem. Phys.*, 2025, **339**, 130701.
99 F. Soltani-nezhad, A. Saljooqi, T. Shamspur and A. Mostafavi, *Polyhedron*, 2019, **165**, 188–196.
100 P. K. Boruah, S. Szunerits, R. Boukherroub and M. R. Das, *Chemosphere*, 2018, **191**, 503–513.
101 T. L. Lemke, D. A. Williams, V. F. Roche and S. W. Zito, *Foye's Principles of Medicinal Chemistry*, seventh edn, 2013.
102 M. Aitken, M. Kleinrock and J. Pritchett, *Global Use of Medicines 2024*, 2024.
103 A. C. Duarte, S. Rodrigues, A. Afonso, A. Nogueira and P. Coutinho, *Pharmaceuticals*, 2022, **15**(4), 393.
104 S. K. Srivastava, *RSC Appl. Interfaces*, 2024, **1**, 340–429.
105 K. Samal, S. Mahapatra and M. Hibzur Ali, *Energy Nexus*, 2022, **6**, 100076.

106 A. O. Oluwole and O. S. Olatunji, *Environ. Sci. Eur.*, 2022, **34**, 5.
107 M. Patel, R. Kumar, K. Kishor, T. Mlsna, C. U. Pittman, Jr. and D. Mohan, *Chem. Rev.*, 2019, **119**, 3510–3673.
108 D. Papagiannaki, M. H. Belay, N. P. F. Gonçalves, E. Robotti, A. Bianco-Prevot, R. Binetti and P. Calza, *Chem. Eng. J. Adv.*, 2022, **10**, 100245.
109 B. S. Rathi, P. S. Kumar and D. N. Vo, *Sci. Total Environ.*, 2021, **797**, 149134.
110 J. Kusi, C. O. Ojewole, A. E. Ojewole and I. Nwi-Mozu, *Antibiotics*, 2022, **11**(6), 821.
111 M. Antonopoulou, C. Kosma, T. Albanis and I. Konstantinou, *Sci. Total Environ.*, 2021, **765**, 144163.
112 S. S. Emmanuel, A. K. Alanazi, A. A. Adesibikan, C. O. Olawoyin, E. T. Abimbola and O. J. Oluwole, Graphene/graphitic-based metal-organic frameworks (MOFs) for photocatalytic degradation of pharmaceutical pollutants: A review, *J. Organomet. Chem.*, 2025, 123915.
113 C. Du, Z. Zhang, S. Tan, G. Yu, H. Chen, L. Zhou, L. Yu, Y. Su, Y. Zhang, F. Deng and S. Wang, *Environ. Res.*, 2021, **200**, 111427.
114 C. Aruljothi, P. Balaji, E. Vaishnavi, T. Pazhanivel and T. Vasuki, *J. Chem. Technol. Biotechnol.*, 2023, **98**, 1908–1917P.
115 D. Qiao, Z. Li, J. Duan and X. He, *Chem. Eng. J.*, 2020, **400**, 125952.
116 C. Du, Z. Zhuo, S. Tan, G. Yu, C. Hong, L. Zhou, L. Yu, Y. Su, Y. Zhang, F. Deng and S. Wang, radiation, *Environ. Res.*, 2021, **200**, 111427.
117 W. Shi, L. Wang, J. Wang, H. Sun, Y. Shi, F. Guo and C. Lu, *Sep. Purif. Technol.*, 2022, **292**, 120987.
118 W.-K. Jo, S. Kumar, M. A. Isaacs, A. F. Lee and S. Karthikeyan, *Appl. Catal., B*, 2017, **201**, 159–168.
119 K. Sekar, W. Jo, S. Kumar, M. Isaacs and A. Lee, Cobalt promoted TiO 2/GO for the photocatalytic degradation of oxytetracycline and Congo Red, *Appl. Catal., B*, 2016, **201**, 159–168, DOI: 10.1016/j.apcatb.2016.08.022.
120 W. W. Anku, E. M. Kiarii, R. Sharma, G. M. Joshi, S. K. Shukla and P. P. Govender, Photocatalytic Degradation of Pharmaceuticals Using Graphene Based Materials, in *A New Generation Material Graphene: Applications in Water Technology*, ed. M. Naushad, Springer, Cham, 2019, pp. 187–208, DOI: 10.1007/978-3-319-75484-0_7.
121 D. T. Sponza and P. Koyuncuoglu, *Clin. Microbiol. Infect. Dis.*, 2019, **4**, 1–10.
122 S. Uruş, M. Çaylar, H. Eskalen and Ş. Özgan, *J. Mater. Sci.: Mater. Electron.*, 2022, **33**, 4314–4329.
123 M. Farhadian, N. Entezami and N. Davari, *Adv. Environ. Sci. Techol.*, 2019, **5**, 55–65.
124 J. Wu, J. Bai, Z. Wang, Z. Liu, Y. Mao, B. Liu and X. Zhu, UV-assisted nitrogen-doped reduced graphene oxide/Fe3O4 composite activated peroxodisulfate degradation of norfloxacin, *Environ. Technol.*, 2022, **43**(1), 95–106.
125 B. Kakavandi, E. Dehghanifard, P. Gholami, M. Noorisepehr and B. MirzaHedayat, *Appl. Surf. Sci.*, 2021, **570**, 151145.
126 Z. Wan and J. Wang, *J. Hazard. Mater.*, 2017, **324**, 653–664.
127 L. Chen, J. Peng, F. Wang, D. Liu, W. Ma, J. Zhang, W. Hu, N. Li, P. Dramou and H. He, *Environ. Sci. Pollut. Res. Int.*, 2021, **28**, 21799–21811.
128 R. Nimshi, J. Vijaya, L. Kennedy, S. Selvamani P, M. Bououdina and P. Sophia, *Ceram. Int.*, 2022, **49**(9), 13762–13773.
129 Y. Zhu, J. Xue, T. Xu, G. He and H. Chen, *J. Mater. Sci.: Mater. Electron.*, 2017, **28**, 1–10.
130 D. Sharma, H. Kumar and S. Kumar, *Appl. Mater. Today*, 2025, **44**, 102706.
131 D. M. Aronoff and E. G. Neilson, *Am. J. Med.*, 2001, **111**, 304–315.
132 G. S. Lipman, F. G. Gaudio, K. P. Eifling, M. A. Ellis, E. M. Otten and C. K. Grissom, *Wilderness Environ. Med.*, 2019, **30**, S33–S46.
133 F. J. Enguita, S. Pereira and A. L. Leitão, *J. Fungi*, 2023, **9**(4), 408.
134 N. Dwivedi and S. Dwivedi, *Bionanotechnology towards Sustainable Management of Environmental Pollution*, 2022.
135 J. Chen, Q. Zhang, W. Chen, U. Farooq, T. Lu, B. Wang, J. Ni, H. Zhang and Z. Qi, *Environ. Sci.: Processes Impacts*, 2023, **25**, 2092–2101.
136 R. Santhosh Kumar, K. Govindan, S. Ramakrishnan, A. R. Kim, J.-S. Kim and D. J. Yoo, *Appl. Surf. Sci.*, 2021, **556**, 149765.
137 A. Castellano-Hinojosa, M. J. Gallardo-Altamirano, J. González-López and A. González-Martínez, *J. Hazard. Mater.*, 2023, **447**, 130818.
138 N. Rashtchi, S. Sobhanardakani, M. Cheraghi, A. Goodarzi and B. Lorestani, *Toxin Rev.*, 2023, **42**, 701–708.
139 C. J. E. Davey, M. H. S. Kraak, A. Praetorius, T. L. Ter Laak and A. P. van Wezel, *Water Res.*, 2022, **222**, 118878.
140 S. Linley, Y. Liu, C. J. Ptacek, D. W. Blowes and F. X. Gu, *ACS Appl. Mater. Interfaces*, 2014, **6**, 4658–4668.
141 M. P. da Silva, A. C. A. de Souza, Á. R. D. Ferreira, P. L. A. do Nascimento, T. J. M. Fraga, J. V. F. L. Cavalcanti, M. G. Ghislandi and M. A. da Motta Sobrinho, *Sci. Rep.*, 2024, **14**, 18916.
142 M. Moztahida, J. Jang, M. Nawaz, S.-R. Lim and D. S. Lee, *Sci. Total Environ.*, 2019, **667**, 741–750.
143 K. Sornalingam, A. McDonagh and J. L. Zhou, *Sci. Total Environ.*, 2016, **550**, 209–224.
144 E. R. Kabir, M. S. Rahman and I. Rahman, *Environ. Toxicol. Pharmacol.*, 2015, **40**, 241–258.
145 Y. Sun, H. Huang, Y. Sun, C. Wang, X.-L. Shi, H.-Y. Hu, T. Kameya and K. Fujie, *Environ. Pollut.*, 2013, **180**, 339–344.
146 A. A. Bayode, S. S. Emmanuel, S. O. Sanni, O. A. Olalekan, O. T. Ore, D. T. Koko and M. O. Omorogie, *Environ. Chem. Ecotoxicol.*, 2024, **6**, 315–337.
147 N. Khadgi, Y. Li, A. R. Upreti, C. Zhang, W. Zhang, Y. Wang and D. Wang, *Photochem. Photobiol.*, 2016, **92**, 238–246.
148 J. M. Thomas, *Proc. A*, 2012, **468**(2143), 1884–1903.
149 C. Trautwein, J. D. Berset, H. Wolschke and K. Kümmerer, *Environ. Int.*, 2014, **70**, 203–212.
150 A. Balakrishnan, M. Sillanpää, M. M. Jacob and D. N. Vo, *Environ. Res.*, 2022, **213**, 113613.

151 A. H. Cheshme Khavar, G. Moussavi, A. Mahjoub, K. Yaghmaeian, V. Srivastava, M. Sillanpää and M. Satari, *Catal. Sci. Technol.*, 2019, **9**, 5819–5837.
152 Z. Akdogan and B. Guven, *Environ. Pollut.*, 2019, **254**, 113011.
153 H. Kye, J. Kim, S. Ju, J. Lee, C. Lim and Y. Yoon, *Heliyon*, 2023, **9**, e14359.
154 A. Ashrafy, A. A. Liza, M. N. Islam, M. M. Billah, S. T. Arafat, M. M. Rahman and S. M. Rahman, *J. Hazard. Mater. Adv.*, 2023, **9**, 100215.
155 K. Barnes, R. Sinclair and D. Watson, *Chemical migration and food contact materials*, Woodhead Publishing, Cambridge, England, 2006.
156 E. Marcharla, S. Vinayagam, L. Gnanasekaran, M. Soto-Moscoso, W.-H. Chen, S. Thanigaivel and S. Ganesan, *Environ. Res.*, 2024, **256**, 119181.
157 L. Jia, L. Liu, Y. Zhang, W. Fu, X. Liu, Q. Wang, M. Tanveer and L. Huang, *Front. Plant Sci.*, 2023, **14**, 1226484.
158 M. Sajjad, Q. Huang, S. Khan, M. A. Khan, Y. Liu, J. Wang, F. Lian, Q. Wang and G. Guo, *Environ. Technol. Innovat.*, 2022, **27**, 102408.
159 A. Bhowmik, G. Saha and S. C. Saha, *Pollutants*, 2024, **4**, 490–497.
160 Y. Li, L. Tao, Q. Wang, F. Wang, G. Li and M. Song, *Environ. Health*, 2023, **1**, 249–257.
161 K. Ziani, C. B. Ioniţă-Mîndrican, M. Mititelu, S. M. Neacşu, C. Negrei, E. Moroşan, D. Drăgănescu and O. T. Preda, *Nutrients*, 2023, **15**(3), 617.
162 L.-C. Wang, J. C.-T. Lin, J.-A. Ye, Y. C. Lim, C.-W. Chen, C.-D. Dong and T.-K. Liu, *Environ. Sci. Technol.*, 2024, **58**, 22391–22404.
163 C. Ompala, J. P. Renault, O. Taché, É. Cournède, S. Devineau and C. Chivas-Joly, *J. Hazard. Mater.*, 2024, **469**, 134083.
164 Z. Chen, X. Liu, W. Wei, H. Chen and B.-J. Ni, *Water Res.*, 2022, **221**, 118820.
165 J. Talvitie, A. Mikola, A. Koistinen and O. Setälä, *Water Res.*, 2017, **123**, 401–407.
166 A. Abdelrasoul and H. Westphalen, in *Water Challenges of an Urbanizing World*, ed. M. Glavan, IntechOpen, Rijeka, 2017, DOI: 10.5772/intechopen.71494.
167 E. Yousif and R. Haddad, *Springerplus*, 2013, **2**, 398.
168 R. Verma, S. Singh, M. K. Dalai, M. Saravanan, V. V. Agrawal and A. K. Srivastava, *Mater. Des.*, 2017, **133**, 10–18.
169 V. UshaVipinachandran, N. K, K. H. B. Haroon, I. Ashokan, A. Sinha, P. Maity and S. K. Bhunia, *Adv. Sustain. Syst.*, 2025, **9**(8), 2500096.
170 P. Devi, A. Soni and J. P. Singh, *J. Polym. Res.*, 2024, **31**, 152.
171 I. Uogintė, S. Pleskytė, M. Skapas, S. Stanionytė and G. Lujanienė, *Int. J. Environ. Sci. Technol.*, 2023, **20**, 9693–9706.
172 R. Kumar, *Adv. Sustain. Syst.*, 2023, **7**, 2300033.
173 *Emerging Materials for Photodegradation and Environmental Remediation of Micro- and Nano-Plastics: Recent Developments and Future Prospects*, ed. L. Singh and S. Kumar, 2025, pp. 281–300.
174 I. Mahmood, S. R. Imadi, K. Shazadi, A. Gul and K. R. Hakeem, *Plant, Soil and Microbes: Volume 1: Implications in Crop Science*, Springer International Publishing, Cham, 2016, pp. 253–269.
175 M. H. Hashimi, R. Hashimi and Q. Ryan, *Asian J. Plant Sci. Res.*, 2020, **5**, 37–47.
176 G. Luna-Sanguino, A. Ruíz-Delgado, A. Tolosana-Moranchel, L. Pascual, S. Malato, A. Bahamonde and M. Faraldos, *Sci. Total Environ.*, 2020, **737**, 140286.
177 T. S. Natarajan, P. K. Gopi, K. Natarajan, H. C. Bajaj and R. J. Tayade, *Water Energy Nexus*, 2021, **4**, 103–112.
178 S. Dehghan, A. J. Jafari, M. FarzadKia, A. Esrafili and R. R. Kalantary, *J. Photochem. Photobiol., A*, 2019, **375**, 280–292.
179 M. Zangiabadi, T. Shamspur, A. Saljooqi and A. Mostafavi, *Appl. Organomet. Chem.*, 2019, **33**, e4813.
180 S. K. Naynava, B. Lorestani, M. Cheraghi, S. Sobhanardakani and B. Shahmoradi, *Water, Air, Soil Pollut.*, 2024, **235**, 274.
181 P. K. Boruah and M. R. Das, *J. Hazard Mater.*, 2020, **385**, 121516.
182 S. Akçağlar, *J. Chem. Technol. Biotechnol.*, 2025, **100**, 138–154.
183 P. Nasiripur, M. Zangiabadi and M. H. Baghersad, *J. Mol. Struct.*, 2021, **1243**, 130875.
184 A. Tabasum, I. A. Bhatti, N. Nadeem, M. Zahid, Z. A. Rehan, T. Hussain and A. Jilani, *Water Sci. Technol.*, 2020, **81**, 178–189.
185 A. Tabasum, M. Alghuthaymi, U. Y. Qazi, I. Shahid, Q. Abbas, R. Javaid, N. Nadeem and M. Zahid, *Plants*, 2020, **10**, 6.
186 M. A. Khoj, N. S. Awwad, H. A. Ibrahium, A. M. Awad and A. F. Hassan, *J. Inorg. Organomet. Polym. Mater.*, 2024, **34**, 3483–3500.
187 M. Dolatabadi, T. Świergosz, C. Wang and S. Ahmadzadeh, *Arab. J. Chem.*, 2023, **16**, 104424.
188 F. Soltani-nezhad, A. Saljooqi, T. Shamspur and A. Mostafavi, *Polyhedron*, 2019, **165**, 188–196.
189 S. S. Affat, *Univ. Thi-Qar J. Sci.*, 2021, **8**, 130–135.
190 H. B. Slama, A. Chenari Bouket, Z. Pourhassan, F. N. Alenezi, A. Silini, H. Cherif-Silini, *et al.*, *Appl. Sci.*, 2021, **11**, 6255.
191 F. Khan, M. S. Khan, S. Kamal, M. Arshad, S. I. Ahmad and S. A. Nami, *J. Mater. Chem. C*, 2020, **8**, 15940–15955.
192 N. A. Al-Rawashdeh, O. Allabadi and M. T. Aljarrah, *ACS Omega*, 2020, **5**, 28046–28055.
193 I. F. Waheed, O. Y. T. Al-Janabi and P. J. Foot, *J. Mol. Liq.*, 2022, **357**, 119084.
194 P. Benjwal, M. Kumar, P. Chamoli and K. K. Kar, *RSC Adv.*, 2015, **5**, 73249–73260.
195 S. Banerjee, P. Benjwal, M. Singh and K. K. Kar, *Appl. Surf. Sci.*, 2018, **439**, 560–568.
196 M. Nadimi, A. Z. Saravani, M. Aroon and A. E. Pirbazari, *Mater. Chem. Phys.*, 2019, **225**, 464–474.
197 S. Bibi, A. Ahmad, M. A. R. Anjum, A. Haleem, M. Siddiq, S. S. Shah and A. Al Kahtani, *J. Environ. Chem. Eng.*, 2021, **9**, 105580.

198 D. P. Ojha, M. K. Joshi and H. J. Kim, *Ceram. Int.*, 2017, **43**, 1290–1297.
199 A. Kumar, L. Rout, L. S. K. Achary, S. K. Mohanty and P. Dash, *New J. Chem.*, 2017, **41**, 10568–10583.
200 A. M. S. Baptisttella, C. M. B. d. Araujo, M. P. da Silva, G. F. O. d. Nascimento, G. R. B. d. Costa, B. F. do Nascimento, M. G. Ghislandi and M. A. d. Motta Sobrinho, *Sep. Sci. Technol.*, 2021, **56**, 425–438.
201 S. Sheshmani, B. Falahat and F. R. Nikmaram, *Int. J. Biol. Macromol.*, 2017, **97**, 671–678.
202 M. M. Khan, S. F. Adil and A. Al-Mayouf, *J. Saudi Chem. Soc.*, 2015, **19**, 462–464.
203 J. Prakash, *Photochem*, 2022, **2**, 651–671.
204 T. Imboon, K. Sugio, J. Khumphon, L. Sridawong, V. M. Gowri, K. Yamada, M. Shima and S. Thongmee, *ACS Omega*, 2025, **10**, 34571–34587.
205 N. Denisov, J. Yoo and P. Schmuki, Effect of different hole scavengers on the photoelectrochemical properties and photocatalytic hydrogen evolution performance of pristine and Pt-decorated TiO2 nanotubes, *Electrochim. Acta*, 2019, **319**, 61–71.
206 J. Treml and K. Šmejkal, Flavonoids as potent scavengers of hydroxyl radicals, *Compr. Rev. Food Sci. Food Saf.*, 2016, **15**(4), 720–738.
207 A. Nandi and I. B. Chatterjee, Scavenging of superoxide radical by ascorbic acid, *J. Biosci.*, 1987, **11**(1), 435–441.
208 S. Banerjee, S. C. Pillai, P. Falaras, K. E. O'Shea, J. A. Byrne and D. D. Dionysiou, *J. Phys. Chem. Lett.*, 2014, **5**, 2543–2554.
209 S. Wu, H. Hu, Y. Lin, J. Zhang and Y. H. Hu, Visible light photocatalytic degradation of tetracycline over TiO_2, *Chem. Eng. J.*, 2020, **382**, 122842.
210 M. El-Kemary, H. El-Shamy and I. El-Mehasseb, Photocatalytic degradation of ciprofloxacin drug in water using ZnO nanoparticles, *J. Lumin.*, 2010, **130**, 2327–2331.
211 S. Yildiz, G. T. Canbaz and H. Mihçiokur, Photocatalytic degradation of oxytetracycline using ZnO catalyst, *Environ. Prog. Sustainable Energy*, 2024, **43**, e14384.
212 P. C. H. D. Castillo, V. Castro-Velázquez and V. Rodríguez-González, Adsorption and photocatalytic-conjugated activity of a chitosan-functionalized titanate coating for the removal of the drug clonazepam from drinking water, *Environ. Sci. Pollut. Res.*, 2025, **32**, 10553–10568.
213 N. Jallouli, K. Elghniji, H. Trabelsi and M. Ksibi, Photocatalytic degradation of paracetamol on TiO_2 nanoparticles and TiO_2/cellulosic fiber under UV and sunlight irradiation, *Arab. J. Chem.*, 2017, **10**, S3640–S3645.
214 A. O. Iuwole and O. S. Olatunji, Enhanced photocatalytic degradation of naproxen in aqueous matrices using reduced graphene oxide (rGO) decorated binary BSO/g-C_3N_4 heterojunction nanocomposites, *Chem. Eng. J. Adv.*, 2022, **12**, 100417.
215 K. Mitamura, H. Narukawa, T. Mizuguchi and K. Shimada, Degradation of estrogen conjugates using titanium dioxide as a photocatalyst, *Anal. Sci.*, 2004, **20**, 3–4.
216 C. F. Carbuloni, J. E. Savoia, J. S. Santos, C. A. Pereira, R. G. Marques, V. A. Ribeiro and A. M. Ferrari, Degradation of metformin in water by TiO_2–ZrO_2 photocatalysis, *J. Environ. Manage.*, 2020, **262**, 110347.
217 I. Uogintė, S. Pleskytė, M. Skapas, S. Stanionytė and G. Lujanienė, Degradation and optimization of microplastic in aqueous solutions with graphene oxide-based nanomaterials, *Int. J. Environ. Sci. Technol.*, 2023, **20**, 9693–9706.
218 Q. Wei and M. Zheng, Enhanced photocatalytic degradation of polyethylene microplastics under simulated sunlight using Fe_3O_4@TiO_2/Ag nanocomposite and optimization *via* response surface methodology, *J. Mater. Sci.: Mater. Electron.*, 2025, **36**, 1675.
219 M. Cruz, C. Gomez, C. J. Duran-Valle, L. M. Pastrana-Martinez, J. L. Faria, A. M. Silva and A. Bahamonde, Bare TiO_2 and graphene oxide–TiO_2 photocatalysts on the degradation of selected pesticides and influence of the water matrix, *Appl. Surf. Sci.*, 2017, **416**, 1013–1021.
220 M. Hassanpour, H. Safardoust-Hojaghan and M. Salavati-Niasari, Degradation of methylene blue and Rhodamine B as water pollutants *via* green synthesized Co_3O_4/ZnO nanocomposite, *J. Mol. Liq.*, 2017, **229**, 293–299.
221 J. T. Adeleke, T. Theivasanthi, M. Thiruppathi, M. Swaminathan, T. Akomolafe and A. B. Alabi, Photocatalytic degradation of methylene blue by ZnO/$NiFe_2O_4$ nanoparticles, *Appl. Surf. Sci.*, 2018, **455**, 195–200.
222 H. A. A. Jamjoum, K. Umar, R. Adnan, M. R. Razali and M. N. Mohamad Ibrahim, Synthesis, Characterization, and Photocatalytic Activities of Graphene Oxide/metal Oxides Nanocomposites: A Review, *Front. Chem.*, 2021, **9**, 752276, DOI: 10.3389/fchem.2021.752276.
223 S. Mandal, S. Mallapur, M. Reddy, J. K. Singh, D.-E. Lee and T. Park, An Overview on Graphene-Metal Oxide Semiconductor Nanocomposite: A Promising Platform for Visible Light Photocatalytic Activity for the Treatment of Various Pollutants in Aqueous Medium, *Molecules*, 2020, **25**, 5380, DOI: 10.3390/molecules25225380.
224 P. M. Visakh and B. Raneesh, *Metal Oxide Nanocomposites: State-of-the-Art and New Challenges*, 2020, DOI: 10.1002/9781119364726.ch1.
225 B. Avar and M. Panigrahi, Synthesis and Characterization of Binary Reduced Graphene Oxide/Metal Oxide Nanocomposites, *Phys. Chem. Solid State*, 2022, **23**, 101–112, DOI: 10.15330/pcss.23.1.101-112.
226 W. Yang, M. Pan, C. Huang, Z. Zhao, J. Wang and H. Zeng, Graphene oxide-based noble-metal nanoparticles composites for environmental application, *Compos. Commun.*, 2021, **24**, 100645, DOI: 10.1016/j.coco.2021.100645.
227 J. Soni, A. Sethiya, N. Sahiba and S. Agarwal, Recent advancements in organic synthesis catalyzed by graphene oxide metal composites as heterogeneous nanocatalysts, *Appl. Organomet. Chem.*, 2021, **35**, e6162, DOI: 10.1002/aoc.6162.
228 S. Ameen, R. Fatima, N. Ullah, A. Tighezza, I. Ali, U. Bilal, S. Saleem and A. S. S. Bilal, Investigation of structural, morphological, thermal, optical, and magnetic properties of graphene-embedded hematite and magnetite

nanocomposites, *Opt. Quant. Electron.*, 2024, **56**, 1–15, DOI: 10.1007/s11082-024-07413-4.

229 S. Ameen, R. Fatima, N. Ullah, A. Tighezza, I. Ali, U. Bilal, S. Saleem and A. S. S. Bilal, Investigation of structural, morphological, thermal, optical, and magnetic properties of graphene-embedded hematite and magnetite nanocomposites, *Opt. Quant. Electron.*, 2024, **56**, 1–15, DOI: 10.1007/s11082-024-07413-4.

230 R. Sharma, H. Kumar, D. Yadav, C. Saini, R. Kumari, G. Kumar, A. B. Kajjam, V. Pandit, M. Ayoub, Saloni, Y. Deswal and A. K. Sharma, Synergistic advancements in nanocomposite design: Harnessing the potential of mixed metal oxide/reduced graphene oxide nanocomposites for multifunctional applications, *J. Energy Storage*, 2024, **93**, 112317, DOI: 10.1016/j.est.2024.112317.

231 G. Ren, H. Han, Y. Wang, S. Liu, J. Zhao, X. Meng and Z. Li, Recent Advances of Photocatalytic Application in Water Treatment: A Review, *Nanomaterials*, 2021, **11**(7), 1804, DOI: 10.3390/nano11071804.

232 O. J. Ajala, J. O. Tijani, M. T. Bankole and A. S. Abdulkareem, A Critical Review on Graphene Oxide Nanostructured material: Properties, Synthesis, Characterization and Application in Water and Wastewater Treatment, *Environ. Nanotechnol. Monit. Manag.*, 2022, **18**, 100673, DOI: 10.1016/j.enmm.2022.100673.